



## Review

# Transmembrane signaling and assembly of the cytochrome $b_6f$ -lipidic charge transfer complex<sup>☆</sup>

S. Saif Hasan<sup>a</sup>, Eiki Yamashita<sup>b</sup>, William A. Cramer<sup>a,\*</sup><sup>a</sup> Department of Biological Sciences, Purdue University, West Lafayette, IN 47907, USA<sup>b</sup> Osaka University, Institute for Protein Research, Suita, Osaka 565-0871, Japan

## ARTICLE INFO

## Article history:

Received 17 December 2012

Received in revised form 27 February 2013

Accepted 6 March 2013

Available online 16 March 2013

## Keywords:

Cytochrome

 $b_6f$  $bc_1$ 

LHC kinase

Transmembrane signaling

Assembly

## ABSTRACT

Structure–function properties of the cytochrome  $b_6f$  complex are sufficiently unique compared to those of the cytochrome  $bc_1$  complex that  $b_6f$  should not be considered a trivially modified  $bc_1$  complex. A unique property of the dimeric  $b_6f$  complex is its involvement in transmembrane signaling associated with the p-side oxidation of plastoquinol. Structure analysis of lipid binding sites in the cyanobacterial  $b_6f$  complex prepared by hydrophobic chromatography shows that the space occupied by the H transmembrane helix in the cytochrome  $b$  subunit of the  $bc_1$  complex is mostly filled by a lipid in the  $b_6f$  crystal structure. It is suggested that this space can be filled by the domain of a transmembrane signaling protein. The identification of lipid sites and likely function defines the intra-membrane conserved central core of the  $b_6f$  complex, consisting of the seven trans-membrane helices of the cytochrome  $b$  and subunit IV polypeptides. The other six TM helices, contributed by cytochrome  $f$ , the iron–sulfur protein, and the four peripheral single span subunits, define a peripheral less conserved domain of the complex. The distribution of conserved and non-conserved domains of each monomer of the complex, and the position and inferred function of a number of the lipids, suggests a model for the sequential assembly in the membrane of the eight subunits of the  $b_6f$  complex, in which the assembly is initiated by formation of the cytochrome  $b_6$ -subunit IV core sub-complex in a monomer unit. Two conformations of the unique lipidic chlorophyll  $a$ , defined in crystal structures, are described, and functions of the outlying  $\beta$ -carotene, a possible ‘latch’ in supercomplex formation, are discussed. This article is part of a Special Issue entitled: Respiratory complex III and related  $bc$  complexes.

© 2013 Elsevier B.V. All rights reserved.

## 1. Introduction

Oxygenic photosynthesis is responsible for conversion of light energy from the sun into chemical energy stored in sugars and ATP [1]. The primary photosynthetic reactions utilizing solar energy involve the oxidation of water by the Photosystem II (PSII) protein complex to release molecular oxygen, electrons and protons (Fig. 1). On the reducing side of PSII, lipophilic plastoquinone (PQ) is reduced to plastoquinol (PQH<sub>2</sub>), which diffuses laterally in the membrane to the cytochrome  $b_6f$  complex (cyt  $b_6f$ ). The protons released by hydrolysis of H<sub>2</sub>O contribute to the transmembrane proton electrochemical gradient,  $\Delta\mu\text{H}^+$ . The  $b_6f$

complex catalyzes PQH<sub>2</sub> deprotonation and oxidation on the lumen (electrochemically positive, p) side of the thylakoid membrane, and PQ reduction and protonation on the stromal (electrochemically negative, n) side. p-side PQH<sub>2</sub> is oxidized by a series of sequential one electron carriers in the high potential electron transport chain consisting of: (i) the membrane bound [2Fe<sub>2</sub>–2S] cluster in the iron–sulfur protein (ISP), usually in coordination with the p-side heme  $b_p$  of the cyt  $b_6$  subunit of the complex, (ii) the cytochrome  $f$  heme in the p-side peripheral domain, (iii) soluble plastocyanin (PC) or cyt  $c_6$ , and (iv) the photosystem I (PSI) reaction center.

2. Structure of the cyt  $b_6f$  complex

The cyt  $b_6f$  complex is a symmetric dimer [2–4] (Fig. 2A, B) that consists of eight transmembrane polypeptide subunits. The  $b_6f$  monomer has two polytopic subunits, cytochrome  $b_6$  (cyt  $b_6$ ) and subunit IV (subIV). Cyt  $b_6$  (~25 kDa, encoded by *petB*) consists of a four-transmembrane helix (TMH) bundle and a short surface helix formed by the N-terminal 28–29 amino acids, which is associated with the n-side membrane surface. TMH helices are labeled A–D. The four TMH of cyt  $b_6$  are connected by loops that are located at the p and n-side membrane–water interfaces. SubIV (~17 kDa, encoded by

**Abbreviations:**  $\beta$ -Car,  $\beta$ -carotene; Chl- $a$ , chlorophyll- $a$ ; Cyt, cytochrome; Em7, midpoint oxidation-reduction potential at pH 7;  $\Delta\mu\text{H}^+$ , transmembrane proton electrochemical potential gradient; n, p-sides, electrochemically negative and positive side of the membrane; PDB, protein data bank; PC, plastocyanin; PQ, plastoquinone; PS, photosystem; subIV, subunit IV of the  $b_6f$  complex; TMH, transmembrane helix

<sup>☆</sup> This article is part of a Special Issue entitled: Respiratory complex III and related  $bc$  complexes.

\* Corresponding author. Tel.: +1 765 494 4956; fax: +1 765 496 1189.

E-mail address: [wacrab@purdue.edu](mailto:wacrab@purdue.edu) (W.A. Cramer).

*petD*) has three TMH (E–F) that form a p-side saddle around the four helix bundle of cyt  $b_6$ . Helix E is located in proximity to the A and B-helix of cyt  $b_6$  while the F and G-TMH span the four helix bundle, close to the B and C-TMH (Fig. 2C). The C-terminus of the E-TMH is separated from the N-terminus of the F-TMH by a distance of  $\sim 40$  Å, which is bridged by the p-side *ef*-loop. This seven TMH assembly forms the polytopic core of the cyt  $b_6f$  complex. Six single TMH arising from individual subunits are arranged in the periphery around the core of the monomeric unit of the complex consisting of the cyt  $b_6$ -subIV subunits: (i) cytochrome *f* (cyt *f*,  $\sim 32$  kDa, encoded by *petA*) and (ii) the Rieske Iron–Sulfur Protein (ISP,  $\sim 19$  kDa, *petC*) each containing a large extrinsic domain on the p-side, attached to one TMH and, (iii–vi) four small (3–4 kDa) subunits. Pet G (gene *petG*), L (gene *petL*), M (gene *petM*) and N (gene *petN*), define a four-helix bundle on the periphery of each monomer of the complex, on the peripheral side opposite the inter-monomer cavity (Fig. 2D).

### 3. Prosthetic groups

The cyt  $b_6f$  monomer has seven prosthetic groups [2,3,5] (Fig. 2A, B). Within the transmembrane region, the B and D TMHs of cyt  $b_6$  are associated with two bis-histidine ligated *b*-hemes ( $b_p$  and  $b_n$ , on the p and n-side). The conserved His86/His187 of the B and D TMHs provides axial coordination to heme  $b_p$  while His100/His202 of the B and D TMHs coordinates heme  $b_n$  [2,3,6]. A unique covalently linked heme  $c_n$  is found to be electronically coupled to heme  $b_n$  through an axial  $H_2O$  or  $OH^-$  ion, on the n-side of the complex [2,3,7,8] (Fig. 3). In the absence of a second axial ligand, heme  $c_n$  is a high spin heme, with a small extinction coefficient in the visible range [9]. Cys35, a conserved residue that is found not only in the photosynthetic cyt  $b_6$  polypeptide but also in the cyt *b* protein of non-photosynthetic firmicutes [10], forms a covalent thioether linkage to heme  $c_n$  (Fig. 3). A chlorophyll-*a* (chl-*a*) and a  $\beta$ -carotene ( $\beta$ -car) molecule are also inserted between the hydrophobic TMHs (Fig. 2B). In the p-side peripheral domain, the cyt *f* polypeptide is covalently linked to a heme molecule (a *c*-type heme) while the ISP extrinsic domain binds one [2Fe–2S] cluster. The midpoint redox potentials at pH 7 of the prosthetic groups involved in electron transfer are summarized in Table 1.

### 4. The inter-monomer cavity

The dimeric structure of cyt  $b_6f$  is organized around an inter-monomer cavity (30 Å high  $\times$  25 Å wide  $\times$  15 Å deep) [2,3,5] (Fig. 2A, B). On the n-side, the cavity is marked by the N-terminal surface helix of cyt  $b_6$  and on the p-side by residues from the A and D-TMH of cyt  $b_6$ . Within the lipid bilayer, the interior of the cavity is lined by amino acids from the A and D-TMH of cyt  $b_6$ , the E-helix of subIV and the ISP TMH. The cavity is considered to provide the space that sequesters the substrate  $PQH_2$  from the membrane bilayer generated by PSII and thus to concentrate the quinol near the p-side oxidation ( $Q_p$ ) site in the complex [11]. The structure around the inter-monomer cavity is stabilized through interactions between residues of cyt  $b_6$  and subIV within the transmembrane region. The Rieske ISP TMH is associated with the cyt *f* TMH of one monomer while its extrinsic domain crosses-over to the other monomer (Fig. 2A), where it interacts with the p-side extrinsic, peripheral domain of cyt *f* and the transmembrane regions of cyt  $b_6$  and subIV. Further stabilization of the dimeric structure is provided by lipid molecules [12] (Fig. 2B) (and see below).

Crystal structures of the cyt  $b_6f$  complex have been obtained from the prokaryotic filamentous cyanobacteria *Nostoc* PCC 7120 [5], *Mastigocladus laminosus* [2,13], and the eukaryotic green alga *Chlamydomonas reinhardtii* [3]. Structures of the  $\sim 250$  residue cyt *f* peripheral domain have been obtained from *C. reinhardtii* [14,15], *Phormidium laminosum* [16], *Brassica rapa* [17–19], while those of the ISP soluble domain have been solved from tryptic fragments of the ISP protein isolated from *Thermosynechococcus elongatus* [20] and *Spinacia oleracea* [21]. While the transmembrane region of the  $b_6f$  complex consists of  $\alpha$ -helices, the N-terminal soluble domain of cyt *f* has an elongate  $\beta$ -sheet structure (Fig. 2A). The covalently linked heme *f* is located in the peripheral sub-domain proximal to the cyt *f* TMH via an unusual ligation of the Tyr1 side chain to the heme Fe, along with an imidazole axial linkage from the side chain of His26 [22]. The entire cyt *f* peripheral domain extends as an elongate 75 Å bowl shaped structure within which the ISP soluble domain is encompassed. The ISP C-terminal peripheral domain is attached to the TMH through a poly-glycine hinge region [2,3,5] (Fig. 2A), which gives the peripheral domain flexibility for motion crucial to catalysis, and consists of  $\beta$ -sheets separated into two smaller domains. The redox active [2Fe–2S]

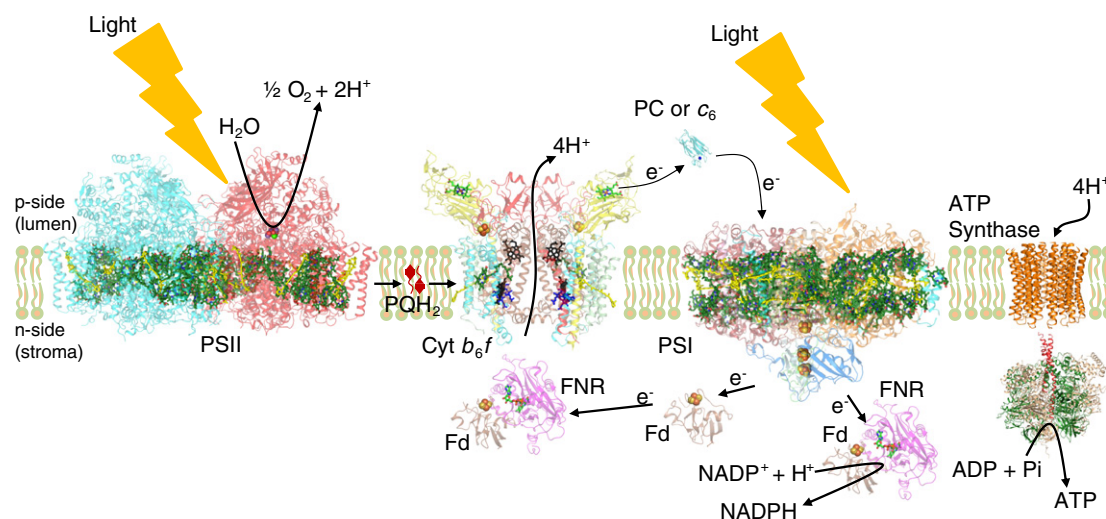


**Fig. 1.** The electron transport chain of oxygenic photosynthesis. Formation of the transmembrane proton electrochemical gradient coupled to the electron transport extending from  $H_2O$  oxidation to  $NADP^+$  reduction, in which  $H^+$  is translocated in the protein complexes of the PSII reaction center and cytochrome  $b_6f$ ; this  $H^+$  gradient is utilized for ATP synthesis by the ATP synthase. PDB accession for structure data: Cyt  $b_6f$  (PDB ID: 2E74), Fd (PDB ID: 1EWY), ferredoxin; FNR (PDB ID: 1EWY), ferredoxin- $NADP^+$ -reductase; PC (PDB ID: 2Q5B), plastocyanin; PSII (PDB ID: 3ARC) and PSI (PDB ID: 1JB0), reaction center complexes.

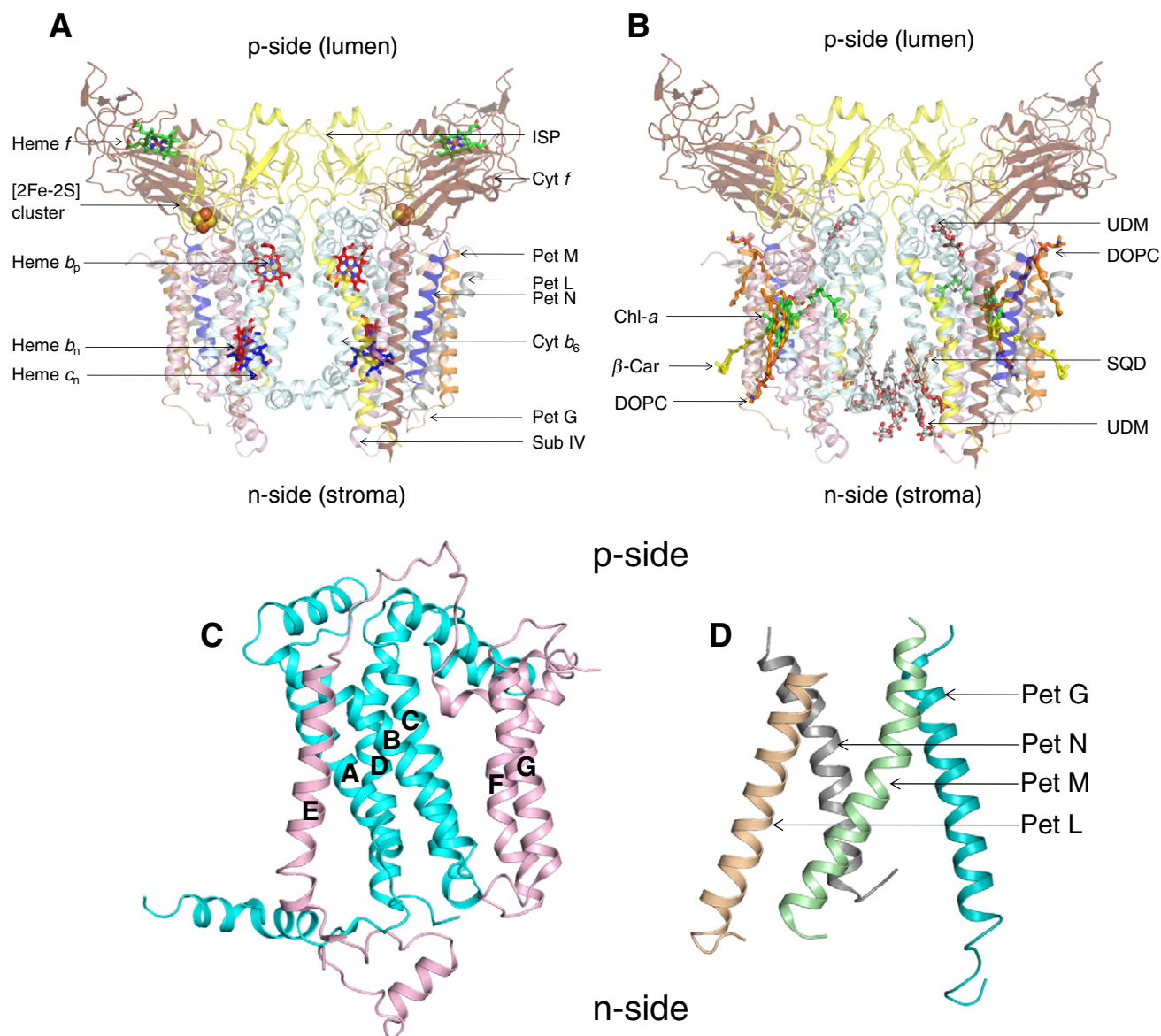


**Fig. 2.** Structure of dimeric  $b_6f$  complex from *M. laminosus* (PDB ID: 2E74): (240,000 MW; per monomer, 8 subunits/7 prosthetic groups; 8 lipids) subunit organization and lipid binding sites. (A) View along membrane plane showing the positions of the 8 subunits. Color code: cytochrome  $f$  (Pet A), yellow; cytochrome  $b_6$  (Pet B), cyan; Rieske [2Fe-2S] protein (Pet C), orange; subunit IV/Pet D (pink), Pet G (teal), Pet L (light brown), Pet M (green) and Pet N (gray). (B) Side view of *M. laminosus*  $b_6f$  complex showing bound lipids, detergents and pigments. (C) Polytopic core of the  $b_6f$  complex. Cyt  $b_6$  (4 TMH, cyan) and subunit IV (3 TMH, pink) form the core of the  $b_6f$  monomer. The cyt  $b_6$  TMH form a four helix bundle. SubIV is organized around the bundle as a bi-partite structure, with the E-helix separated from the F and G TMH. (D) Peripheral four helix bundle formed by the small Pet subunits, Pet G, L, M and N. In addition, including ferredoxin-NADP $^{+}$ -reductase (FNR), which may mediate electron transfer from PSI to cyt  $b_6f$ . (Fig. 1) In addition, there are four soluble subunits that associate with purified  $b_6f$  complex from plant or algal sources, but have not been seen in the crystal structures and have presumably dissociated and been lost during crystallization: the Pet P polypeptide seen in cyanobacteria, the light-harvesting LHClI chlorophyll protein kinase Stt7-STN7, the correlated phosphatase, and the PetO nuclear-encoded phosphorylatable subunit.

cluster is linked to the subdomain extrinsic to the ISP TMH. His109 and His129 side chains coordinate the outer Fe atom of the cluster while the inner Fe is linked to Cys107 and Cys127.

### 5. Sequence and structure similarity between cyt $b_6f$ and $bc_1$ complexes

Cyt  $b_6f$  and  $bc_1$  constitute the family of cytochrome  $bc$  complexes [23]. Cyt  $b_6f$  and  $bc_1$  share several structural features. The transmembrane quinol oxidoreductase and proton pumping function of cyt  $b_6f$  is performed by the homologous cyt  $bc_1$  complex in photosynthetic and denitrifying bacteria and in the membranes of mitochondria (Fig. 4A). Cyt  $b_6$  has four TMH (A–D), as does the cyt  $b$  ( $bc_1$ ) N-terminal domain. However, subIV has three TMH (E–G), one short of the four TMH found

in the C-terminal domain of cyt  $b$ . The C-terminal 8th helix, labeled “H” in cyt  $b$  ( $bc_1$ ), is absent from subIV. Structurally, the cyt  $b_6$  subunit is arranged as the N-terminal domain four TMH of cyt  $b$ . SubIV has a slightly altered structure (Fig. 4B) due to insertion of the chl- $a$  molecule between the F and G TMH, and the absence of helix H from subIV.

Sequence similarity between the single helix subunits of cyt  $b_6f$  and  $bc_1$  is limited. The ISP subunit has a significant conservation of 47–61% in the sequence only in the cluster binding sub-domain [21,24]. Structurally, the overall fold of the ISP soluble domain and TMH is very similar between  $b_6f$  and  $bc_1$  except in the N-terminal region that constitutes the TMH on the n-side. In  $b_6f$ , the TMH of ISP is bent while that in the  $bc_1$  complex forms a straight  $\alpha$ -helix [3]. There is no conservation between the sequence and structure of the  $b_6f$  cyt  $f$  and the analogous cytochrome  $c_1$  (cyt  $c_1$ ) of  $bc_1$ . Both polypeptides provide a covalently linked



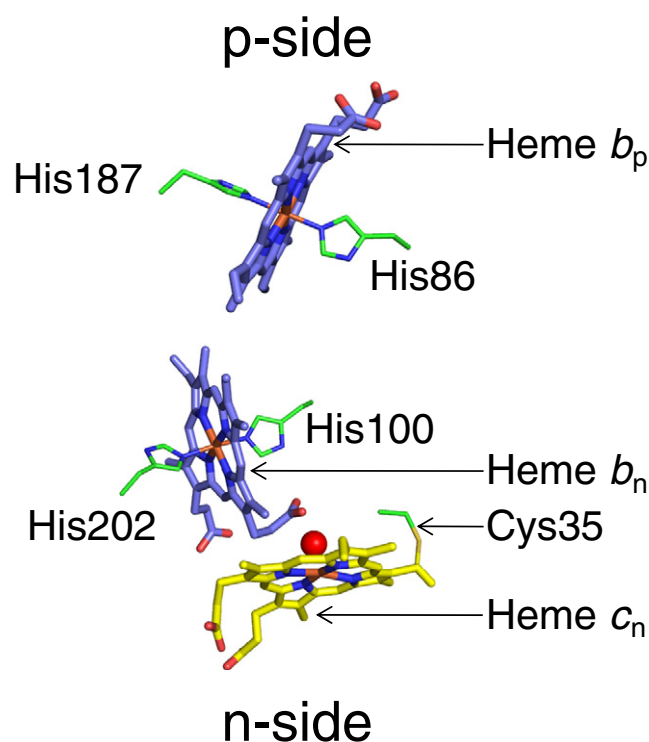


**Fig. 3.** Transmembrane heme organization within *cyt b<sub>6</sub>f*. Three hemes, *b<sub>p</sub>*, *b<sub>n</sub>* and *c<sub>n</sub>*, are located within the *b<sub>6</sub>f* hydrophobic core. Hemes *b<sub>p</sub>* and *b<sub>n</sub>* are axially ligated by histidines from *cyt b<sub>6</sub>*. Heme *c<sub>n</sub>*, a unique heme without an amino acid axial ligand, is linked to a conserved Cys35 residue of *cyt b<sub>6</sub>*, and is axially ligated by a water or hydroxide molecule (red sphere).

heme that functions as the electron acceptor for the ISP [2Fe–2S] cluster, and hence, show convergent evolution [19]. Structurally, *cyt f* consists of an elongated  $\beta$ -sheet extrinsic domain and one TMH, while the *cyt c<sub>1</sub>* soluble domain has a globular,  $\alpha$ -helical arrangement (reviewed recently in [25]).

## 6. Function similarity between *cyt b<sub>6</sub>f* and *bc<sub>1</sub>* complexes

*Cyt b<sub>6</sub>f* and *bc<sub>1</sub>* complexes act as a plastoquinol:plastocyanin and ubiquinol:cytochrome *c* oxidoreductase, respectively, to catalyze a “Q-cycle” [26–32]. However, the mechanism of this cycle differs in the two complexes because of the presence of the heme *c<sub>n</sub>*, possibly FNR, and of the PSI cyclic pathway in the *b<sub>6</sub>f* complex [10]. The enzyme FNR, found in association with the *b<sub>6</sub>f* complex on the n-side [33], may donate an electron from NADPH to the *Q<sub>n</sub>*-site to complete the reduction of the plastoquinone, thereby decreasing the number of p-side PQH<sub>2</sub>-oxidation events required for the n-side reduction of PQ. The association of *b<sub>6</sub>f* with FNR may be an important evolutionary adaptation with significant kinetic consequences as the p-site quinol

deprotonation reaction constitutes the rate limiting step in the activity of *cyt bc* complexes, with an activation energy of 32 kJ/mol [34,35]. By providing an alternate route for electron delivery to the *Q<sub>n</sub>*-site, FNR may contribute to acceleration of the rate of photosynthetic electron transfer.

## 7. Differences between *cyt b<sub>6</sub>f* and *bc<sub>1</sub>* complexes

(i) In addition to the linear electron transport (LET) pathway, an additional pathway, the PSI cyclic pathway operates in oxygenic photosynthesis in a feedback mechanism to transfer electrons from the reducing n-side of PSI to the quinone pool via an n-side entry to *cyt b<sub>6</sub>f* and/or complex I (Fig. 1), thereby balancing redox poise and regulating the ATP level needed for carbon fixation [10]. There is no corresponding pathway in the *bc<sub>1</sub>* complex. (ii) Heme *c<sub>n</sub>*, which occupies much of the n-side quinone binding niche of the *bc<sub>1</sub>* complex, is electronically coupled to heme *b<sub>n</sub>* from which it is separated by 4 Å [2,3,5]. (iii) The small Pet subunits of *cyt b<sub>6</sub>f*, Pet G, L, M and N, have no homologous substitutes in the *bc<sub>1</sub>* complex [2,3]. Instead, their position is occupied by lipids in *bc<sub>1</sub>* [36]. (iv) *Cyt bc<sub>1</sub>* also has several extrinsic polypeptides, both soluble and transmembrane, that are found only in the eukaryotic complex [37]. These subunits are absent in the prokaryotic *bc<sub>1</sub>* [38] and the photosynthetic *b<sub>6</sub>f* complexes [2,3]. (v) The *b<sub>6</sub>f* complex contains three more prosthetic groups than *bc<sub>1</sub>*. While both complexes have hemes *b<sub>p</sub>* and *b<sub>n</sub>* in the transmembrane region and a [2Fe–2S] cluster and a covalently linked heme in the soluble domains, the unique heme *c<sub>n</sub>*, chl-*a* and  $\beta$ -car are not found in the *bc<sub>1</sub>* complex [39]. (vi) The architecture of the *Q<sub>p</sub>* and *Q<sub>n</sub>* sites also differs between the complexes due to the presence of a chl-*a* and the unique heme *c<sub>n</sub>* in the *b<sub>6</sub>f* complex. On the p-side, the heterocyclic chlorin ring of the chl-*a* molecule is located between the F and G TMH of subIV (Fig. 2B) while its long phytyl-tail passes into the portal of quinone entry that leads to the *Q<sub>p</sub>*-site in *b<sub>6</sub>f* [5,11]. This portal is formed by residues from the C-helix of *cyt b<sub>6</sub>* and the F-helix of subIV and measures 12–15 Å in cross-section. The absence of chl-*a* from the *bc<sub>1</sub>* complex enlarges the *Q<sub>p</sub>*-portal, which may have effects on the residence time of the substrate quinol within the *Q<sub>p</sub>*-site, thereby providing a major difference between structure and kinetics on the p-side of *cyt b<sub>6</sub>f* and *bc<sub>1</sub>*. On the n-side, heme *c<sub>n</sub>* (Fig. 3) is located at the *Q<sub>n</sub>*-site, with its open axial position facing the inter-monomer cavity. Crystallographic studies have implicated this open axial position as the quinone binding site in *b<sub>6</sub>f* [13]. Compared to the *Q<sub>n</sub>*-site of *bc<sub>1</sub>* that consists of an amino acid environment leading to heme *b<sub>n</sub>*, the *Q<sub>n</sub>*-site of *b<sub>6</sub>f* provides greater access to the substrate quinone from the inter-monomer cavity. This structural difference has an important implication in reducing the selectivity and efficiency of inhibitor binding to the *Q<sub>n</sub>*-site (discussed below), again providing for major structural, kinetic and equilibrium related differences between *b<sub>6</sub>f* and *bc<sub>1</sub>*. In summarizing the differences between the two sets of complexes, it can be said that the *b<sub>6</sub>f* complex is not a trivially modified *bc<sub>1</sub>* complex.

## 8. Lipids associated with the *b<sub>6</sub>f* complex

Membrane proteins depend on internal integral lipids for structural stability and biological activity [40–42]. The role of lipids in stabilizing the structure of membrane proteins, or even inducing structural changes within proteins has been investigated by methods that are sensitive to changes in secondary and tertiary structure, thermal stability assays using, for example, enzymatic activity, that provide information about the functional dependence of the protein on lipid content [40,43].

It is now well documented that successful crystallization of a large number of membrane proteins depends on the presence of stabilizing lipids, as in the case of the photosynthetic light harvesting complex [44], bacteriorhodopsin [45], GPCRs [46] and aquaporin [47]. High resolution crystal structures of membrane proteins provided evidence for specific lipid–protein interactions, as deduced from the presence of well-defined lipid binding sites occupied by ordered lipids, both on

**Table 1**  
Subunits of the *cyt b<sub>6</sub>f* complex (*M. l.*, *M. lamosus*, *C. r.*, *C. reinhardtii*) [39].

Subunit	MW (kDa)	MW (kDa)	pI	pI	<i>E<sub>m7</sub></i> (mV)
	<i>M. l.</i>	<i>C. r.</i>	<i>M. l.</i>	<i>C. r.</i>	
Cyt <i>f</i> (1 heme)	32.273	31.249	6.7	8.3	+350–380
Cyt <i>b<sub>6</sub></i> (3 hemes)	24.712	24.165	9.0	8.8	(–50, <i>b<sub>n</sub></i> ); –50 to –150, <i>b<sub>p</sub></i> ; +100, <i>c<sub>n</sub></i>
ISP [2Fe–2S]	19.295	18.333	6.8	5.8	+300–320
SubIV	17.528	17.295	8.1	6.6	–
PetG	4.058	3.984	4.5	4.4	–
PetM	3.841	4.036	10.4	4.3	–
PetL	3.530	3.436	10.2	9.5	–
PetN	3.304	3.282	5.7	6.0	–

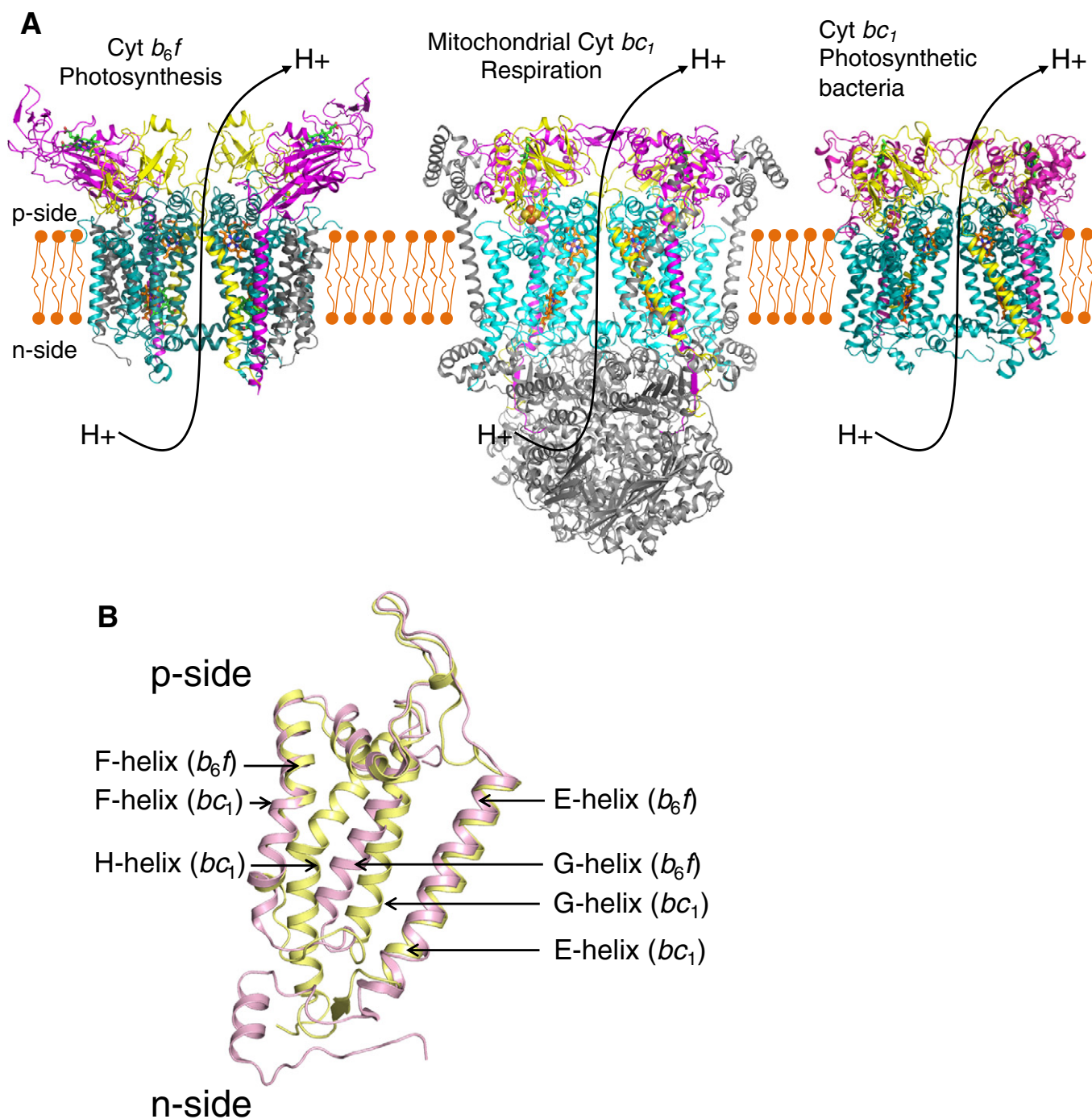


**Fig. 4.** Family of cyt  $bc$  complexes. (A) Cyt  $b_6f$  and the  $bc_1$  complex of mitochondria and anoxygenic photosynthetic bacteria constitute the cyt  $bc$  family. The transmembrane core (teal) of the  $bc$  complexes is highly conserved. The complexes catalyze quinone reduction–protonation and quinol deprotonation–oxidation, respectively, on the electrochemically negative and positive sides of the membrane to generate the proton electrochemical potential gradient. (B) Structural differences in the core: C-terminal domain of the  $bc_1$  cyt  $b$  subunit (4 TMH, yellow) has a TMH organization that differs from subIV (3 TMH, pink) of the  $b_6f$  complex, although amino acid sequences are highly conserved.

the surface and within folded polypeptides. The class of membrane proteins that represents the largest number of well-defined lipid binding sites observed structurally is that of the hetero-oligomeric complexes that consist of distinct polypeptide subunits [48,49]. Membrane protein complexes are assembled from protein components of different sizes and amino acid compositions. The problem of packing the components together to form a stable membrane protein complex is solved by the incorporation of lipid molecules, which interact with the surrounding protein environment, mainly through Van der Waals interactions [50,51].

Due to the non-specific nature of these interactions, it may be possible to substitute a natural lipid with a synthetic lipid without affecting biological function [52–54]. During the process of purification, natural lipids may also be replaced by detergent molecules that serve as synthetic structural and functional analogs of lipids [48]. Due to the smaller volume occupied by a single tail, detergents tend to form micelles, and not bilayers like lipids [40]. The physico-chemical similarity between the properties of lipids and detergents has implications for the identification of lipid binding sites [48,49]. The presence of a crystallographically

well defined site with a bound detergent molecule is considered to mark the position of a natural lipid. Weakly bound lipids may be replaced by detergent molecules, especially at the surface of membrane proteins. Therefore, the analysis of lipid binding sites in membrane proteins is inclusive of sites occupied by natural lipids, synthetic lipids as well as ordered detergent molecules.

Prior to elucidation of the cyt *b<sub>6</sub>f* crystal structure, a role of lipids in the structure had been inferred through biochemical studies [55,56]. Successful crystallization of the cyanobacterial cyt *b<sub>6</sub>f* complex to obtain highly diffracting crystals required the addition of a synthetic lipid to the purified and delipidated *b<sub>6</sub>f* preparation. Addition of the neutral lipid dioleoylphosphatidylcholine (DOPC) improved diffraction quality of *b<sub>6</sub>f* crystals from 11 Å to 3 Å [2,50]. Purification of the *b<sub>6</sub>f* complex from the eukaryotic alga *C. reinhardtii* for successful crystallization was carried out under mild conditions of metal-affinity chromatography that did not remove lipids from the complex [3]. Elucidation of the structure of cyt *b<sub>6</sub>f* from *M. lamosus* showed the presence of a total of 4 lipids and 4 detergent bound sites within the transmembrane domain, in addition to the hydrophobic photosynthetic pigments chl-*a* and  $\beta$ -carotene (Fig. 2A, B).

The use of hydrophobic chromatography allowed manipulation of lipid content in the eight lipid binding sites of cyt *b<sub>6</sub>f* (Fig. 2B). The finding that the hydrophobic space occupied by the eighth transmembrane helix of the respiratory and anoxic photosynthetic cytochrome *bc<sub>1</sub>* complex is occupied by a lipid and a chlorophyll in the *b<sub>6</sub>f* complex raises the question of the pressure in evolution that led to this change [12,57,58]. The question is posed of the function of the lipid substitution in relation to the evolutionary change between the eight and seven helix structures of the cyt *b* polypeptide [57]. Based on the known n-side activation of the light harvesting chlorophyll protein kinase by p-side plastoquinol [58], one possibility is that the change was directed by the selective advantage of p- to n-side transmembrane signaling functions in *b<sub>6</sub>f*, with the lipid either mediating this function, or substituting for the TMH of a signaling protein lost during purification and/or crystallization.

## 9. Assembly of the hetero-oligomeric cyt *b<sub>6</sub>f* complex

As discussed above, the active dimeric cyt *b<sub>6</sub>f* complex consists of at least 8 distinct transmembrane gene products (cyt *f*, cyt *b<sub>6</sub>*, Rieske ISP, subIV, Pet G, L, M and N), along with 7 tightly bound prosthetic groups (hemes *f*, *b<sub>p</sub>*, *b<sub>n</sub>* and *c<sub>n</sub>*, [2Fe–2S] cluster, chl-*a* and  $\beta$ -car) (Fig. 2A, B). The genes for the subunits do not constitute a single operon. The cyt *b<sub>6</sub>* gene (*petB*) and the subIV gene (*petD*) are under the genetic control of a single promoter, as the *petBD* operon [59,60]. In prokaryotes, the ISP gene (*petC*) and the cyt *f* gene (*petA*) are also organized into an operon, the *petCA* operon. Hence, the transcription of the four major subunits is expected to be genetically co-ordinated. However, the four peripheral subunits, Pet G, L, M and N, are not encoded by genes that belong to an operon. Genetic control and coordination of the Pet G, L, M and N synthesis are not well understood.

Mutagenesis studies have provided information about the sequence of events that lead to the assembly of the dimeric cyt *b<sub>6</sub>f* complex [61–69]. Heme binding has been suggested to be an important event in stabilization of the cyt *b<sub>6</sub>f* component polypeptides. In the absence of bound heme moieties, the cyt *b<sub>6</sub>* and cyt *f* polypeptides are highly sensitive to proteases [63,64]. An analysis of the cyt *b<sub>6</sub>f* crystal structures shows that the cyt *b<sub>6</sub>* hemes *b<sub>p</sub>* and *b<sub>n</sub>* are involved in structural stabilization to the cyt *b<sub>6</sub>* polypeptide. Axial coordination to the hemes *b<sub>p</sub>* and *b<sub>n</sub>* is provided by His86/His187 and His100/His202 respectively of the cyt *b<sub>6</sub>* polypeptide, which leads to its folding into a compact four helix bundle [2,3]. Heme-mediated stabilization of the cyt *f* subunit occurs via an unusual ligation of the heme via the Tyr1 residue side-chain of the mature cyt *f* polypeptide [18]. Crystal structures of the isolated cyt *f* extrinsic domain and of the intact dimeric cyt *b<sub>6</sub>f* complex show virtually no structural differences between the cyt *f* extrinsic domain. Hence,

heme binding is an important event in the folding and stabilization of the subunits of the cyt *b<sub>6</sub>f* complex.

The hetero-oligomeric nature of the *b<sub>6</sub>f* complex requires the presence of lipids to enhance and strengthen protein–protein interactions between non-identical subunits [52]. Lipids present on the surface and between polypeptide subunits provide cross-linking interactions that contribute to stability of the complex. As discussed elsewhere [12], crystal structures of *b<sub>6</sub>f* show well-defined lipid, detergent and lipidic pigment binding sites. The organization of lipidic molecules within the *b<sub>6</sub>f* complex provides clues to the process of assembly. Given the close interactions between the distinct polypeptides and the integral association of prosthetic groups and lipids with the folded polypeptides, it is important to determine the mode of cyt *b<sub>6</sub>f* assembly in the thylakoid membrane, both in terms of the order in which various subunits are assembled and the stage(s) of insertion of prosthetic groups.

Assembly of a functional cyt *b<sub>6</sub>f* complex dimer would require coordination in time of synthesis of the various subunits and proximity of the synthesized products to ensure that all necessary polypeptides are available to assemble into the functional complex. On the basis of the genetic organization of cyt *b<sub>6</sub>f* and crystal structures of the purified dimeric complex from the cyanobacteria *M. lamosus* (PDB IDs: 1VF5, 2E74) [2,13] and *Nostoc* PCC 7120 (PDB ID: 2ZT9) [5], and *C. reinhardtii* (PDB ID: 1Q90) [3], a model is proposed to explain the sequence of events that lead to the formation of the dimeric cyt *b<sub>6</sub>f* complex in thylakoid membranes. The first step is considered to involve the transcriptional activation of the *petBD* operon that encodes the polytopic cyt *b<sub>6</sub>* and subIV subunits of *b<sub>6</sub>f* that form the core. Following transcription, the mRNA is translated into the cyt *b<sub>6</sub>* and subIV polypeptides that undergo co-insertion into the membrane to form the polytopic monomeric core of the cyt *b<sub>6</sub>f* complex (Fig. 5, step 1). Dimerization of the polytopic monomer is expected to follow its assembly. As seen in the crystal structures of the *b<sub>6</sub>f* complex, lipids, and detergents that mark physiological lipid binding sites act as cross-linkers to stabilize monomer–monomer interactions at the interface of the dimer. Three lipid sites mediate inter-monomer interactions, viz., (i) p-side lipid, mimicked by the synthetic lipid DOPC (Fig. 5, step B, DOPC lipid shown as red sticks) in the *M. lamosus* cyt *b<sub>6</sub>f* structure (PDB ID: 1VF5) located at the opening of the inter-monomer cavity, and (ii, iii) two n-side UDM detergent occupied sites (Fig. 5, step A, UDM detergent shown as red/white sticks) that interact with the cyt *b<sub>6</sub>* N-terminus of one monomer and the cyt *b<sub>6</sub>* D TMH of the other monomer in *M. lamosus* cyt *b<sub>6</sub>f* (PDB ID: 2E74) (Fig. 5, step C). The ISP and cyt *f* polypeptides are expected to be co-inserted into the thylakoid membrane to form an ISP–cyt *f* sub-complex (Fig. 5, step D). The interaction between the two polypeptides is strengthened on the n-side by the native acidic sulfolipid that interacts with basic residues from the transmembrane helices of ISP and cyt *f*. On the p-side, the ISP–cyt *f* interaction is mediated by another lipid binding site. A detergent and a photosynthetic pigment eicosane were modeled into this site in crystal structures of the *b<sub>6</sub>f* complex from cyanobacteria (PDB IDs: 2E74, 2ZT9) and *C. reinhardtii* (PDB ID: 1Q90). Van der Waals interactions stabilize the interaction between lipid in the p-side site and the residues of the ISP and cyt *f* TMH. This ISP–cyt *f* sub-complex then interacts with the cyt *b<sub>6</sub>*–subIV polytopic core nucleus to form a cyt *b<sub>6</sub>*–subIV–ISP–cyt *f* sub-complex. As discussed elsewhere [12], the sulfolipid and the ligand in the p-side lipid site contribute to the association through Van der Waals interactions with residues from the polytopic core. Biochemical evidence supports the existence of an ISP–cyt *f* sub-complex in spinach [70]. The proposed model explains the existence of these smaller complexes as a consequence of proximity between the genes that encode these subunits, which allows for coordination in transcription, translation, membrane insertion and assembly.

The four small subunits of the cyt *b<sub>6</sub>f* complex, Pet G, L, M and N, are organized into a four helix bundle in the structure of the *b<sub>6</sub>f* complex [2,3,5,13]. Pet L, M and N form a  $\beta$ -car binding site. The sequence conservation of these subunits is low. Pet G, the subunit with the highest



degree of sequence conservation does not interact with the  $\beta$ -car [12,71]. Since these subunits are encoded by genes that are separated by large distances, the assembly process would require a long-range communication for coordination between genetic transcription, translation, membrane insertion and assembly. The structure of the  $b_6f$  complex shows that on the n-side, the extrinsic portion of these subunits consists of basic amino acid residues [11,72]. Based on the *cis*-positive rule [73] and the short length of the Pet subunit helices that span the hydrophobic membrane only once, it has been suggested that they are inserted spontaneously into the membrane [72]. It is expected that organization of the Pet subunits around the  $\beta$ -car molecule leads to the formation of the four helix bundle (Fig. 5, step 5). Assembly of the PetGLMN sub-complex may take place independently on the periphery of the cyt  $b_6f$  polytopic core. Mutagenesis studies have shown that Pet G and Pet N, which show relatively high sequence conservation, are essential to the stability of the dimeric  $b_6f$  complex [71,74,75].

The crystal structure of the cyt  $b_6f$  complex shows a clear separation between the polytopic core domain and the peripheral domain that consists of single helix subunits [12]. It is noted that the PetGLMN sub-complex may interact with the ISP-cyt  $f$  sub-complex (Fig. 5, step 6), leading to the formation of a peripheral sub-complex that interacts with the polytopic core, which eventually forms the hetero-oligomeric, fully functional cyt  $b_6f$  complex (Fig. 5, step 7).

## 10. Cyt $b_6f$ and super-complex formation

Elucidation of the structural organization of cyt  $bc$  complexes provided an understanding of the function performed by these quinone oxidoreductases in energy transduction. Sequence conservation of the transmembrane core subunits [6] was found to extend to the structure cyt  $bc$  complexes, between the cyt  $b$  polypeptide of the  $bc_1$  complex and the cyt  $b_6$ /subIV polypeptides of the cyt  $b_6f$  complex (discussed above). A significant and conserved structural feature relates to the organization of the p-side quinol oxidation ( $Q_p$ ) site. It has been demonstrated that the deprotonation of the semiquinone intermediate within the  $Q_p$ -site is mediated by the Glu residue of the conserved PEWY sequence located on the *ef*-loop [76–78]. In the cyt  $bc_1$  complex (PDB ID: 3CX5) [79], the *ef*-loop is inserted between the F and G TMH of the cyt  $b$  subunit (Fig. 6, left panel). Stabilization of the  $Q_p$ -site architecture depends on the 8th C-terminal “H” TMH of the cyt  $b$  subunit in the  $bc_1$  complex. The helix is inserted in the space between the F and G helices and hence, stabilizes the inter-helix space that is required for the insertion of the *ef*-loop. A very similar structural arrangement of the  $Q_p$ -site is observed in the  $b_6f$  complex (Fig. 6, right panel). However, it has been noted previously that an unusual evolutionary structural difference between the cyt  $b_6f$  and  $bc_1$  complexes is seen in the organization of the cyt  $b$  polypeptide [12,57]. The ‘H’ TMH, which performs an

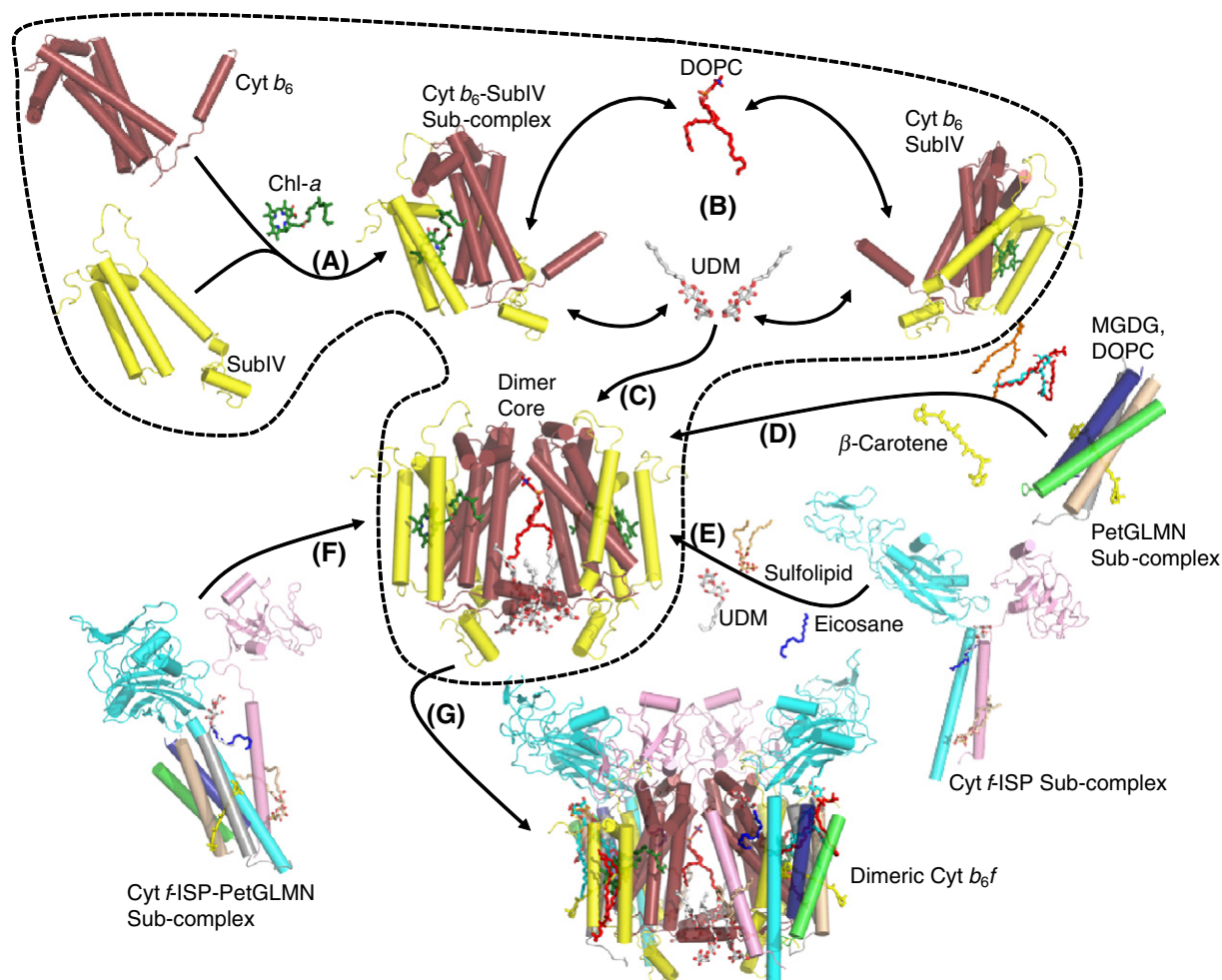


**Fig. 5.** Proposed model for assembly of the cyt  $b_6f$  complex. (Step A) The first step involves the assembly of the monomeric polytopic core of cyt  $b_6$  and subIV. (Step B) The monomeric polytopic core then undergoes dimerization, mediated by the cross-linking interactions of lipids (DOPC, shown as red sticks; UDM shown as red/white sticks), which leads to the formation of the dimeric cyt  $b_6$ -subIV polytopic core (Step C). Formation of the ISP-cyt  $f$  sub-complex takes place via the stabilizing interactions of lipids (Step D). Assembly of the PetGLMN sub-complex takes place around the  $\beta$ -carotene molecule (Step E). Interaction of the PetGLMN sub-complex with the core polytopic core takes place via the  $\beta$ -carotene and lipids (sulfolipid, DOPC, MGDG). Alternatively, formation of an ISP-cyt  $f$ -PetGLMN sub-complex may take place prior to interaction with the dimeric core (Step F). (Step G) Interaction of the peripheral sub-complex with the dimeric core would lead to the formation of the fully assembled, functional dimeric cyt  $b_6f$  complex.

important role of stabilizing the niche for the catalytically important *ef*-loop, is absent from the photosynthetic *cyt b<sub>6f</sub>* complex. As demonstrated, the niche of the missing H TMH is occupied by a lipid and a chl-*a* molecule in the *cyt b<sub>6f</sub>* complex.

### 11. Protein-to-lipid substitution: structure-driven evolutionary modification

Why should a transmembrane helix be replaced by a lipid and a lipid-like chl-*a* molecule? A possible explanation may lie in the pathway of state transitions, which is unique to photosynthesis (Fig. 7) [80]. Photosynthetic state transitions balance the redox poise of the plastoquinone (PQ)/plastoquinol (PQH<sub>2</sub>) pool within the thylakoid membrane. The Photosystem-II (PSII) reaction center utilizes solar energy to catalyze the reduction of PQ to PQH<sub>2</sub> (Fig. 7A). The reduced PQH<sub>2</sub> moiety then diffuses to the *cyt b<sub>6f</sub>* complex, where it undergoes oxidation within the Q<sub>p</sub>-site. Based on studies performed on the *cyt bc<sub>1</sub>* complex, quinol oxidation within the Q<sub>p</sub>-site of the *cyt b<sub>6f</sub>* complex is expected to constitute the rate limiting step in the photosynthetic electron transport chain. As a result, PQH<sub>2</sub>/PQ redox poise shifts to a predominantly reduced state (Fig. 7B). To restore balance, an enzyme identified as the LHCII kinase Stt7 in *C. reinhardtii*, is activated [81,82]. The LHCII kinase phosphorylates the accessory antenna LHC molecules associated with the PSII reaction center, causing their dissociation and migration to photosystem I (PSI). In the absence of LHC molecules, the efficiency of light harvesting and catalysis of PQ reduction by PSII is significantly diminished (Fig. 7C). PQH<sub>2</sub> consumption by the *cyt b<sub>6f</sub>* complex is not affected, and hence, redox balance is restored in the PQ/PQH<sub>2</sub> pool. Mutagenesis experiments have shown that the *cyt b<sub>6f</sub>* complex acts as the sensor of the quinone pool redox state [58]. Binding of PQH<sub>2</sub> within the Q<sub>p</sub>-site generates a signal that activates the LHCII kinase. Biochemical studies of the Stt7 kinase in *C. reinhardtii* show that the kinase has a membrane spanning domain along with an extrinsic domain on n-side of the thylakoid membrane [81,82]. Catalytic activity of the LHCII kinase resides in the extrinsic domain, and is activated by PQH<sub>2</sub> binding within *cyt b<sub>6f</sub>* on the p-side of the membrane. The kinase activating signal has to be transduced

across the hydrophobic bilayer. The exact mechanism by which PQH<sub>2</sub> binding generates the signal and the identity of the signal are presently unknown.

### 12. LHCII kinase activation: putative mechanism

A comparative analysis of the *cyt b<sub>6f</sub>* crystal structures from cyanobacteria (PDB IDs: 2E74, 2ZT9) and *C. reinhardtii* (PDB ID: 1Q90) shows an interesting structural feature that may be relevant to transmembrane signal transduction to activate state transitions. The chl-*a* chlorin-ring is inserted between the F and G TMH of subIV (Fig. 8). The phytol-tail of chl-*a* passes through the portal that leads into the Q<sub>p</sub>-site for substrate binding. The phytol-tail of the chl-*a* has different conformations in the crystal structures of *cyt b<sub>6f</sub>* obtained from cyanobacteria (PDB IDs: 2E74, 2ZT9) and *C. reinhardtii* (PDB ID: 1Q90). In the cyanobacterial *cyt b<sub>6f</sub>* complex, the chl-*a* phytol tail is wrapped around the F TMH while in the *cyt b<sub>6f</sub>* structure from *C. reinhardtii*, the phytol-tail is located proximal to the C TMH (Fig. 8). The alternate positions indicate potential flexibility in the chl-*a* phytol-tail. It is proposed that upon binding of the natural substrate plastoquinol-9 within the Q<sub>p</sub>-portal of *cyt b<sub>6f</sub>*, the 45 carbon long isoprenoid tail of plastoquinol-9 molecule displaces the chl-*a* phytol-tail, thereby modifying the interaction between chl-*a* and the 'F' TMH (Fig. 9). It is proposed that changes in the chl-*a*/F TMH interaction generate a signal that is transduced to the n-side of the *cyt b<sub>6f</sub>* complex, either directly through the 'F' TMH or by a combinatorial mechanism that involves the 'F' and lipid substituting for the 'H' TMH. The 'F' TMH is the prime candidate for signal transduction as it provides a direct physical connection between the substrate binding Q<sub>p</sub>-site on the p-side and the n-side surface of the *cyt b<sub>6f</sub>* complex.

It is significant to note that no structure is available for the isolated, purified LHCII kinase. Biochemical evidence is not available to determine the binding site for the kinase on the *cyt b<sub>6f</sub>* complex. It is possible that the lipid bound between the 'F' and 'G' TMH of *cyt b<sub>6f</sub>* actually represents the LHCII kinase binding site. Crystallographic evidence can be

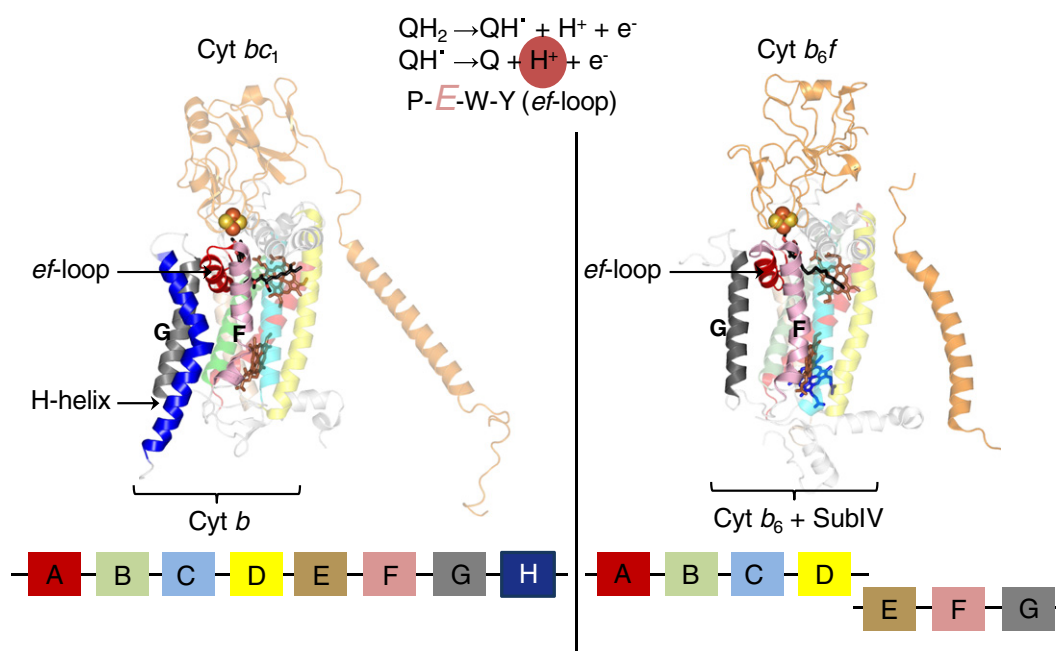


**Fig. 6.** Organization of the Q<sub>p</sub>-site in cytochrome *bc* complexes. The *ef*-loop bears the conserved PEWY sequence, whose Glu residue is involved in the second deprotonation reaction (highlighted in reaction sequence) of the substrate within the Q<sub>p</sub>-site. Left panel: In the *cyt bc<sub>1</sub>* complex (PDB ID: 3CX5), the *ef*-loop is inserted between the F and G transmembrane helices of the 8 helix *cyt b* polypeptide (shown in block diagram at the bottom). The space between the F and G TMH is stabilized by the H TMH of *cyt b*. Right panel: In the *cyt b<sub>6f</sub>* complex (PDB ID: 2E74), the 'H' TMH is absent from the subIV polypeptide (shown as block diagram). This niche is occupied by a lipid and a chlorophyll-*a* molecule.



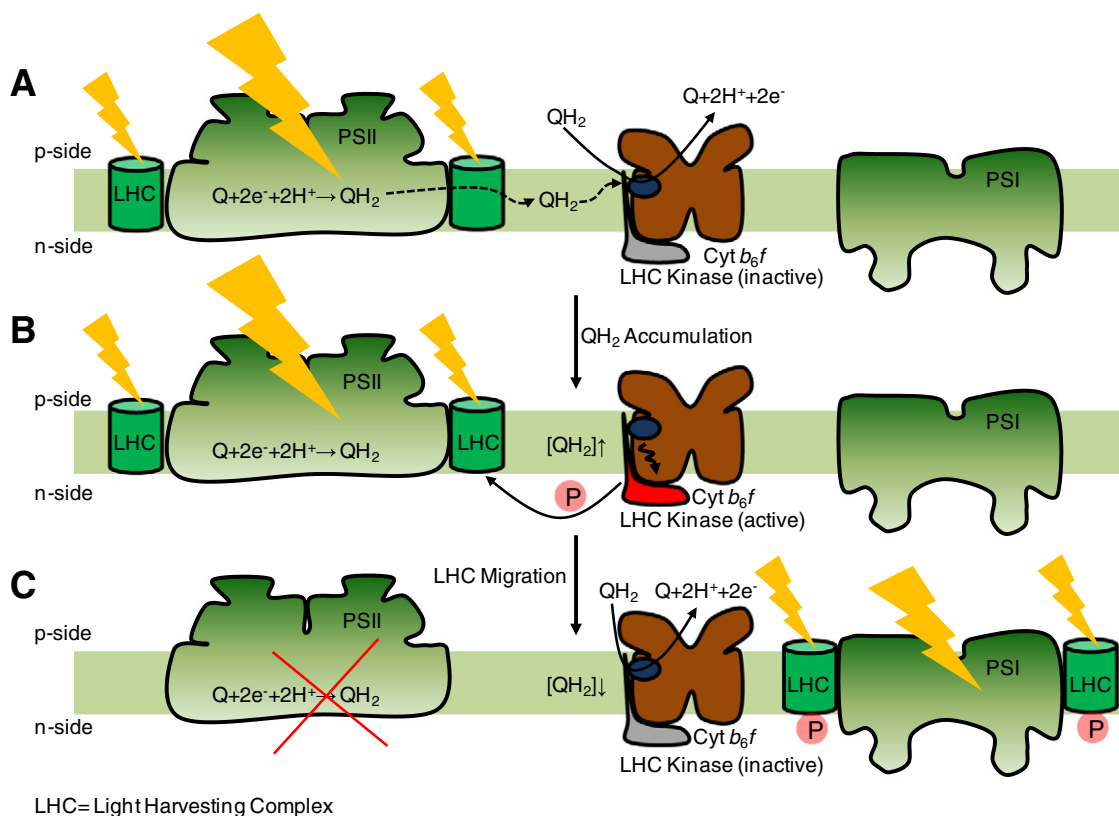


**Fig. 7.** Photosynthetic state transitions. (A) The photosystem II (PSII) reaction center complex utilizes light energy harvested by accessory light harvesting complex II (LHC) molecules to reduce plastoquinone (PQ) to plastoquinol ( $PQH_2$ ).  $PQH_2$  undergoes diffusion to the  $Q_p$ -site (blue circle) of the  $cyt\ b_6f$  complex (brown cartoon), where it undergoes oxidation. (B) Slow  $PQH_2$  oxidation by  $cyt\ b_6f$  causes  $PQH_2$  accumulation in the thylakoid membrane, which activates the LHCII kinase (shown in red). (C) In the phosphorylated state, LHC molecules migrate to photosystem I (PSI), thereby reducing the efficiency of PQ reduction by PSII. As  $PQH_2$  consumption by  $cyt\ b_6f$  is not affected, a redox balance is restored in the quinone pool, which inactivates the LHCII kinase (shown in gray).

obtained from cyanobacterial crystal structures of the  $cyt\ b_6f$  complex [5,13] in which DOPC, a non-physiological lipid, is able to bind in the niche. Hence, the lipid binding site between the 'F' and 'G' TMH is not expected to have a very high affinity for lipids. This inference is further supported by the crystal structure of the  $cyt\ b_6f$  complex obtained from *C. reinhardtii* [3]. A long, tubular electron density is observed in the binding niche between the F and G helices, which may belong to lipid present at a low occupancy (Fig. 10). Based on these observations of an exchangeable lipid, it is proposed that the niche formed between the F and G TMH may represent the binding site for the LHCII kinase (Fig. 11). In this model, the presence of the lipid may represent a state in which the  $cyt\ b_6f$ -LHCII kinase association has not been established. Formation of the  $cyt\ b_6f$ -LHCII kinase super-complex would be accompanied by the replacement of the n-side lipid by the transmembrane domain of the LHCII kinase. The LHCII kinase would interact with the  $Q_p$ -site and the F TMH of  $cyt\ b_6f$ . According to the proposed model, replacement of the H TMH of the  $cyt\ b$  polypeptide is explained by the need to generate the binding site for the LHCII kinase [83].

### 13. Structure-linked role of $\beta$ -carotene in $cyt\ b_6f$ complex

The model of LHCII kinase binding and activation assigns a structural role to the photosynthetic pigment chl-*a*, instead of a photochemical function. This is a unique role that is not commonly observed. In the  $cyt\ b_6f$  complex, in addition to the chl-*a* molecule, one  $\beta$ -car is inserted into the periphery of the complex, in between the peripheral Pet subunits, as described elsewhere [2,3] and discussed above. Biological systems that harvest light, such as photosystems and light harvesting complex proteins, utilize chlorophyll molecules to capture light and initiate photochemistry. However, in the excited triplet state,

the chlorophyll molecule has the potential to transfer energy to molecular oxygen, leading to the formation of harmful reactive oxygen species [83].  $\beta$ -Car molecules are utilized as quenchers in such

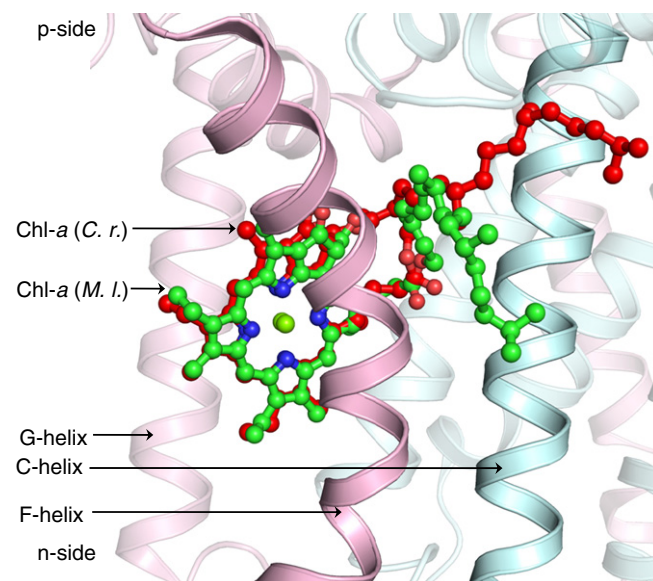


**Fig. 8.** Alternate conformations of the chl-*a* phytol-tail in  $cyt\ b_6f$ . The chl-*a* chlorin-ring is inserted between the F and G TMH of subIV (light pink) while the tail is inserted between the F TMH and the C TMH of  $cyt\ b_6$  (pale cyan). In the crystal structure of  $cyt\ b_6f$  (PDB ID: 2E74) from the cyanobacterium *M. laminosus*, the chl-*a* phytol-tail (green) is wrapped around the F TMH while in the structure obtained from *C. reinhardtii*, the chl-*a* phytol-tail (red) is located proximal to the C TMH.

biological systems to dissipate energy from the potentially harmful excited triplet state of chlorophyll. However, the separation between the chl-*a* and the  $\beta$ -car molecule within the cyt *b<sub>6</sub>f* monomer is 14 Å, which is significantly larger than a 4 Å distance that would allow efficient wave-function overlap [84]. It has been suggested that the energy transfer does take place between the chl-*a* and  $\beta$ -car of cyt *b<sub>6</sub>f* via an oxygen-channel [85,86]. However, experimental demonstration of such a channel remains elusive. As an alternative function, the  $\beta$ -car molecule is thought to perform two structural roles [12,57]. The  $\beta$ -car molecule may mediate assembly of the hetero-oligomeric cyt *b<sub>6</sub>f* complex by providing a scaffold for the organization of the PetGLMN sub-complex. Additionally, it has been suggested that the  $\beta$ -car molecule may function as a molecular antenna that mediates the search for other photosynthetic complexes, such as PSI, and then serves as a latch to mediate the formation of a cyt *b<sub>6</sub>f*-PSI super-complex [3,12]. The isolation of an enzymatically functional cyt *b<sub>6</sub>f*-PSI super-complex has recently been reported from *C. reinhardtii* thylakoid membranes [87]. While the models proposed in the present discussion suggest structural functions for the photosynthetic pigments chl-*a* and  $\beta$ -car, the problem of the large 14 Å separation between the pigment molecules in the cyt *b<sub>6</sub>f* complex still remains. In the absence of a  $\beta$ -car mediated pathway to channel energy from the excited chl-*a* molecule, the cyt *b<sub>6</sub>f* complex is prone to generate reactive harmful species that may cause oxidation of biological molecules. It is expected that a mechanism for energy dissipation from the chl-*a* moiety of cyt *b<sub>6</sub>f* must be operational under in-vivo conditions of photosynthetic electron transfer.

Structural studies of the cyt *b<sub>6</sub>f* complex have so far been performed in isolation with crystallization grade purity [50]. While crystallographic studies of the isolated cyt *b<sub>6</sub>f* complex have yielded valuable information, it has not been possible to study the interactions of the cyt *b<sub>6</sub>f* complex

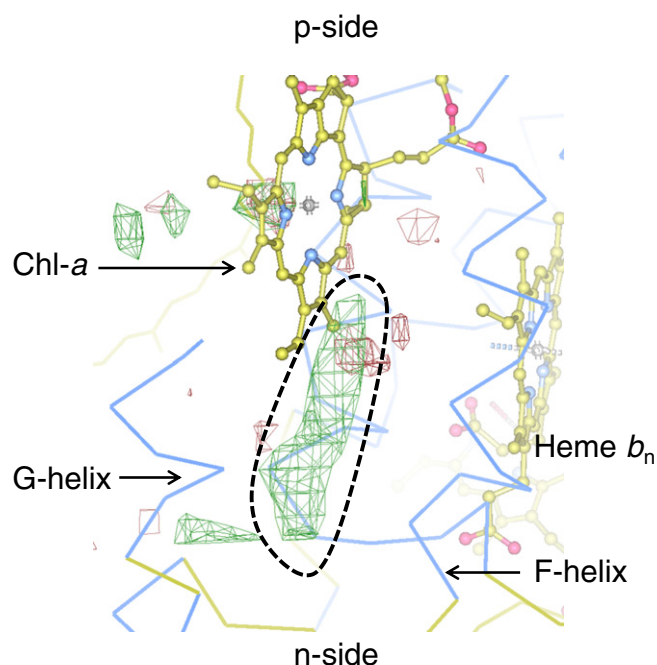


**Fig. 10.** Potential lipid binding site in cyt *b<sub>6</sub>f* complex of *C. reinhardtii*. The cyt *b<sub>6</sub>f* structure (PDB ID: 1Q90) was obtained in the presence of native lipids. Residual electron density is shown as green mesh (highlighted by broken black line) between the Fo–Fc map (3.0  $\sigma$ ). The electron density corresponds to the n-side lipid in the cyanobacterial cyt *b<sub>6</sub>f* complexes from *M. lamosus* (PDB ID: 2E74) and *Nostoc* PCC 7120 (PDB ID: 2ZT9). The electron density map was obtained from the Electron Density Server [96].

with other membrane proteins, such as the photosystems. Within the thylakoid membrane, photosystems, cyt *b<sub>6</sub>f* and LHC complexes do not operate in isolation. Interaction between the large hetero-oligomeric membrane bound complexes mediates physiologically relevant photochemistry and electrochemistry. On these lines, it is possible that the chl-*a* molecule of the cyt *b<sub>6</sub>f* complex is quenched by a  $\beta$ -car from another membrane bound photosynthetic protein, such as a photosystem or an LHC molecule. Such an interaction would require close interaction between cyt *b<sub>6</sub>f* and other membrane bound proteins. With the elucidation of the existence of a cyt *b<sub>6</sub>f*-PSI super-complex [87], evidence has been presented for physical association between the hetero-oligomeric photosynthetic complexes. An analysis of the crystal structures of Photosystems I [88] and II [89,90] and of the light harvesting complex II [91] shows that peripheral carotenoids are ubiquitous in these complexes (Fig. 12). Hence, it is possible that the formation of a super-complex of the cyt *b<sub>6</sub>f* complex not only mediates metabolic processes, but also provides the necessary pathway for quenching of the chl-*a* excited state within the *b<sub>6</sub>f* complex.

#### 14. Selectivity (and the lack thereof) in the *Q<sub>n</sub>*-site of cyt *b<sub>6</sub>f* complex

A useful tool in studies of electron transfer through the hemes and [2Fe–2S] cluster prosthetic groups of cyt *bc* complexes has been the use of specific quinone analog inhibitors [92–94]. Inhibitors approximately simulate the binding properties of the natural substrate to occupy the *Q<sub>p</sub>* and *Q<sub>n</sub>* sites of quinol oxidation and quinone reduction on the p and n-sides of cyt *bc* complexes. In the presence of inhibitors, electron transfer is inhibited through the cyt *bc* complexes. Specific inhibitors have been designed to block defined pathways of electron transfer. As a result, characterization of inhibitors has been performed according to their specific role in blocking the process of electron transfer. With regard to the cyt *bc<sub>1</sub>* complex [94], class I inhibitors include stigmatellin

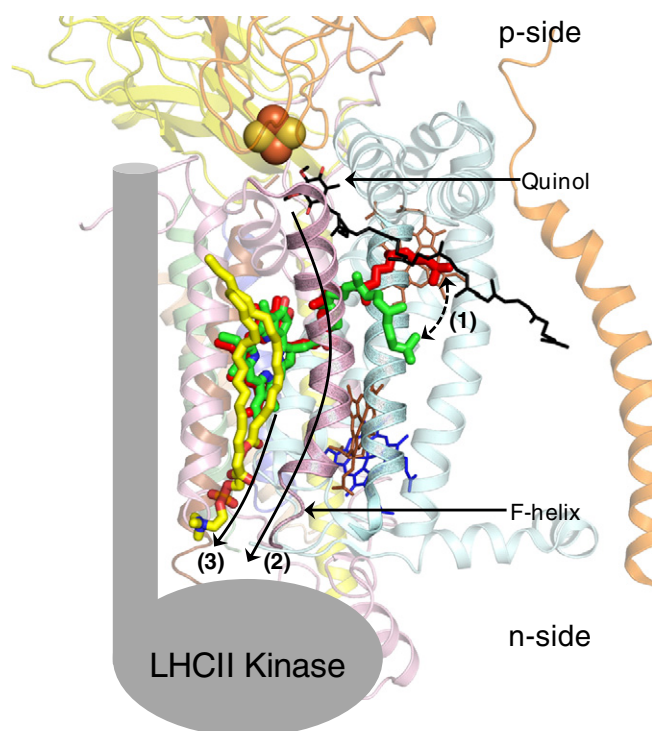


**Fig. 9.** Proposed mechanism of chl-*a* mediated signal transduction in the cyt *b<sub>6</sub>f* complex (PDB ID: 2E74) for activation of photosynthetic state transitions. (Step 1) Binding of the natural substrate plastoquinol (black/red sticks) within the *Q<sub>p</sub>*-site displaces the chl-*a* phytol-tail (displacement shown as broken line with arrows) due to interaction with the long isoprenoid tail of the plastoquinol molecule. The displacement event generates a signal that is transduced to the n-side of the complex either (Step 2) via the F TMH or (Step 3) through a combination of the F TMH and the n-side lipid (yellow) present between the F and G TMH. The LHCII kinase is shown (gray) in cartoon format.



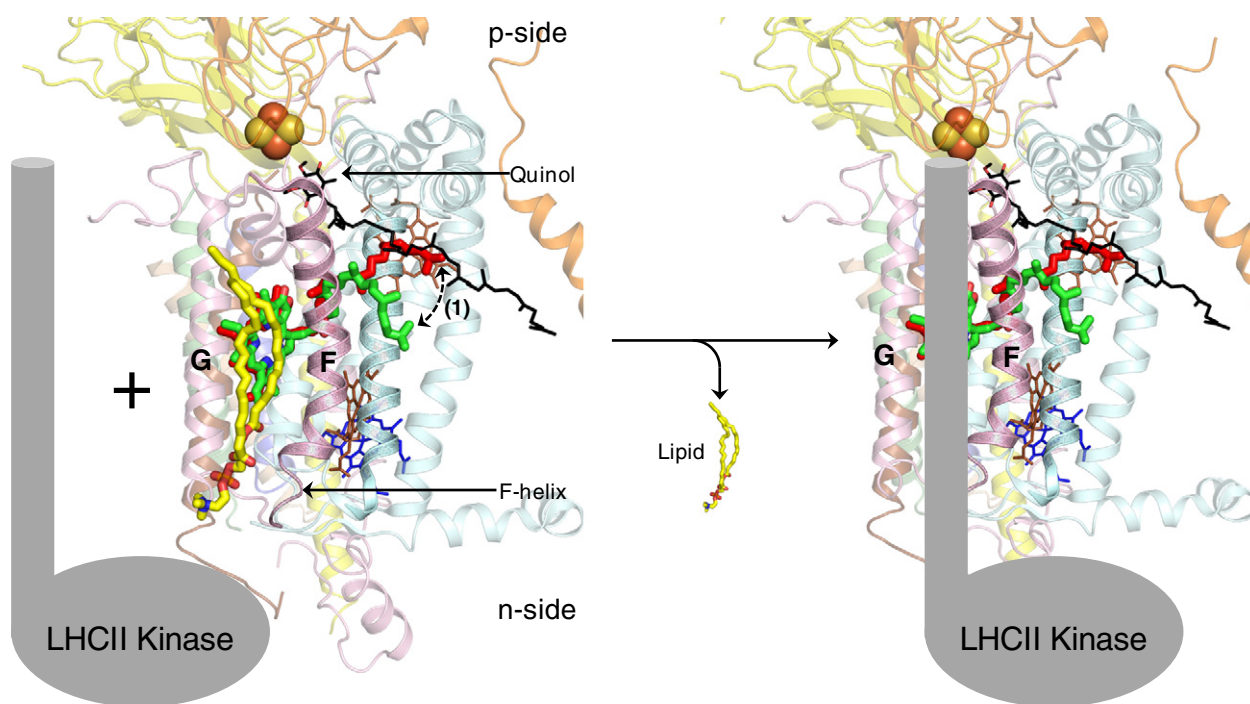


**Fig. 11.** The lipidic mechanism of cyt  $b_6f$ -LHCII kinase super-complex formation. It is proposed that the lipid DOPC (yellow/red/blue sticks) is bound weakly in the niche formed between the F and G TMH, which represents the LHCII kinase (shown as cartoon, gray) binding site. Recruitment of the LHCII kinase to the cyt  $b_6f$  complex and binding results in the replacement of the lipid from the inter-helix niche.

and 5-n-undecyl-6-hydroxy-4,7-dioxobenzothioale (UHDBT) that bind within the  $Q_p$ -site and interact with the ISP subunit. The binding of class I inhibitors has been characterized to occur in a 'pocket' removed from heme  $b_p$  and within H-bond distance of an ISP histidine residue. On the other hand, class II inhibitors include myxothiazole,  $\beta$ -methoxyacrylate stilbene (MOA-stilbene) and famoxadone that bind close to heme  $b_p$  and do not interact with the ISP protein significantly, with the exception of famoxadone. Together, the class I and II inhibitors comprise the p-side quinone analog inhibitors that prevent quinol oxidation within the  $Q_p$ -portal of the cyt  $bc_1$  complex. On the n-side of the cyt  $bc_1$  complex, one of the most well-characterized and

potent inhibitors is antimycin-A. The inhibitor antimycin-A prevents the n-side reaction, i.e., reduction of quinone to quinol bound at the  $Q_n$ -site of the cyt  $bc_1$  complex. Distinction of quinone analog inhibitors as p and n-side specific agents is possible from crystallographic studies of cyt  $bc_1$  complex [38,94,95]. Crystallographic studies of the purified cyt  $b_6f$  complex from the cyanobacterium *M. laminosus* present a different situation [13]. Tridecyl-stigmatellin (TDS), an analog of the cyt  $bc_1$  p-side inhibitor stigmatellin was used for co-crystallization studies. As expected from previous studies, TDS was found to bind at the  $Q_p$ -site within the cyt  $b_6f$  complex. Surprisingly, electron density for the chromone ring of TDS was also observed on the n-side, bound

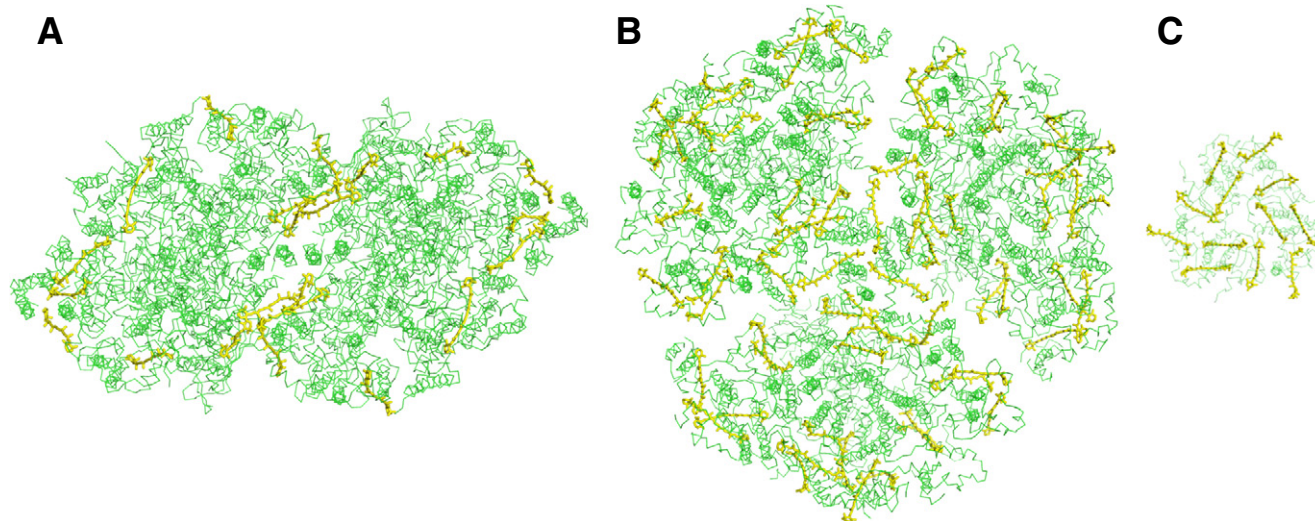


**Fig. 12.** Arrangement of  $\beta$ -carotene in the major photosynthetic integral membrane protein complexes (A) photosystem II (PDB ID: 3ARC), (B) photosystem I (PDB ID: 1JB0) and light harvesting complex II (PDB ID: 2BHW). The  $\beta$ -car molecules are shown as yellow sticks while the polypeptides are represented as thin green ribbons. The  $\beta$ -car molecules are located on the periphery of the complexes, providing potential interaction sites for the chl- $a$  of cyt  $b_6f$ . All three complexes are viewed along the normal to the membrane plane. For simplicity, other prosthetic groups have been omitted.



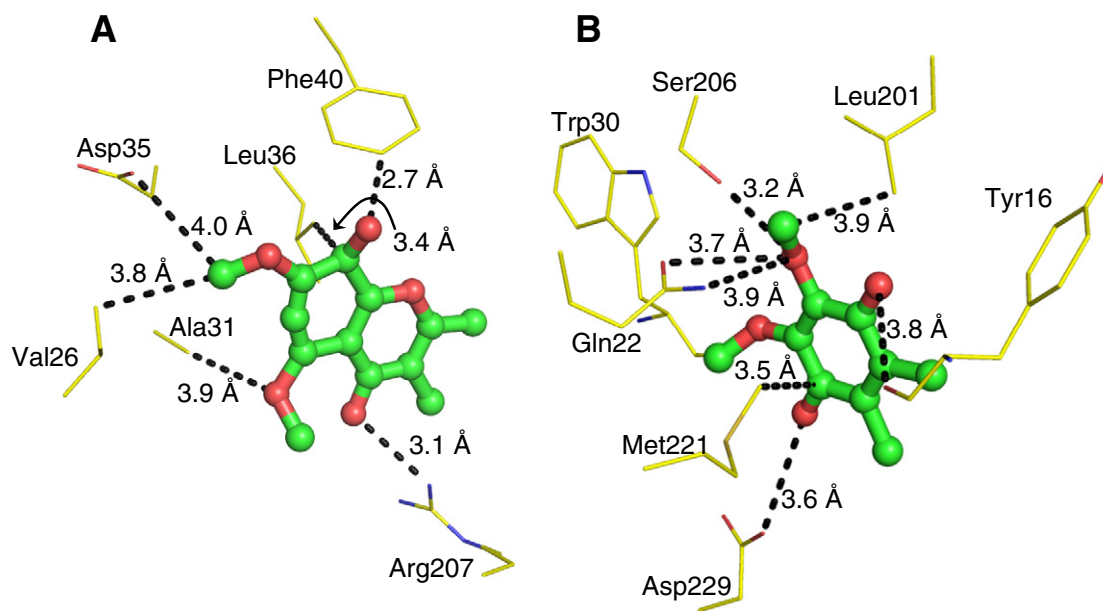


**Fig. 13.** Binding of ligands to the Q<sub>n</sub>-site of cyt bc complexes and the role of the protein environment in selectivity. (A) In the cyt b<sub>6</sub>f structure (PDB ID: 2E76) obtained from the cyanobacterium *M. laminosus*, the majority of the interactions to the quinone analog inhibitor TDS (green/red ball and stick model) are contributed through non-specific Van der Waals interaction. (B) On the other hand, binding of the natural ligand ubiquinone-6 (green/red ball and stick model) to the cyt b<sub>c1</sub> complex (PDB ID: 1KB9) Q<sub>n</sub>-site is mediated by polar interactions. For simplicity, the hydrophobic tails of TDS and ubiquinone-6 have been omitted.

axially to the unique heme c<sub>n</sub>. Binding of TDS at the Q<sub>n</sub>-site of cyt b<sub>6</sub>f indicates that selectivity of inhibitor binding at the Q<sub>n</sub>-site may be less well defined in cyt b<sub>6</sub>f compared to the cyt b<sub>c1</sub> complex.

An analysis of the polypeptide environment around the Q<sub>n</sub>-site of the cyt b<sub>6</sub>f complex provides an explanation for the limited selectivity of inhibitor binding (Fig. 13). The Q<sub>n</sub>-site in the cyt b<sub>6</sub>f complex consists of a heme b<sub>n</sub>/c<sub>n</sub> couple [13]. The presence of heme c<sub>n</sub> extends the binding site of the substrate quinone farther away from the protein environment, into the inter-monomer cavity of the cyt b<sub>6</sub>f dimer. Using the TDS molecule bound axially to heme c<sub>n</sub> as a marker for the natural quinone, it is found that only six amino acids lie within an interaction distance (i.e., within 4.0 Å) of the TDS chromone ring (Fig. 13A). Val26 of cyt b<sub>6</sub> and Ala31, Asp35, Leu36 and Phe40 interact with the TDS chromone ring through Van der Waals interaction. Arg207 of cyt b<sub>6</sub> forms the only selective hydrogen bond interaction with the TDS chromone ring. In contrast, in the cyt b<sub>c1</sub> complex (PDB ID: 1KB9) [36], the ring of the ubiquinone-6 molecule bound at the Q<sub>n</sub>-site interacts with seven residues from the cyt b polypeptide within a distance of 4.0 Å. Tyr16, Gln22, Trp30, Ser206 and Asp229 form polar interactions with the quinone ring while Leu201 and Met221 interact via Van der Waals interactions (Fig. 13B). Hence, selectivity is larger in the cyt b<sub>c1</sub> complex due to the larger fraction of selective polar interactions. This structural feature may also explain the observation that no quinone analog inhibitor for the cyt b<sub>6</sub>f Q<sub>n</sub>-site has been found to be comparable in efficiency to antimycin bound at the Q<sub>n</sub>-site of cyt b<sub>c1</sub> [92]. It is inferred that binding of ligands and quinone analog inhibitors at the Q<sub>n</sub>-site is less selective in the b<sub>6</sub>f complex than in the b<sub>c1</sub> complex, mainly due to fewer interactions.

## Acknowledgments

Financial support was provided by NIH-GM038323 (WAC), Henry Koffler Distinguished Professorship (WAC) and Purdue University (SSH).

## References

- [1] N. Nelson, A. Ben-Shem, The complex architecture of oxygenic photosynthesis, *Nat. Rev. Mol. Cell Biol.* 5 (2004) 971–982.
- [2] G. Kurisu, H. Zhang, J.L. Smith, W.A. Cramer, Structure of the cytochrome b<sub>6</sub>f complex of oxygenic photosynthesis: tuning the cavity, *Science* 302 (2003) 1009–1014.
- [3] D. Stroebel, Y. Choquet, J.L. Popot, D. Picot, An atypical haem in the cytochrome b<sub>6</sub>f complex, *Nature* 426 (2003) 413–418.
- [4] J.F. Allen, Cytochrome b<sub>6</sub>f: structure for signalling and vectorial metabolism, *Trends Plant Sci.* 9 (2004) 130–137.
- [5] D. Baniulis, E. Yamashita, J.P. Whitelegge, A.I. Zatsman, M.P. Hendrich, S.S. Hasan, C.M. Ryan, W.A. Cramer, Structure–function, stability, and chemical modification of the cyanobacterial cytochrome b<sub>6</sub>f complex from *Nostoc* sp. PCC 7120, *J. Biol. Chem.* 284 (2009) 9861–9869.
- [6] W.R. Widger, W.A. Cramer, R.G. Herrmann, A. Trebst, Sequence homology and structural similarity between cytochrome b of mitochondrial complex III and the chloroplast b<sub>6</sub>-f complex: position of the cytochrome b hemes in the membrane, *Proc. Natl. Acad. Sci. U. S. A.* 81 (1984) 674–678.
- [7] A.I. Zatsman, H. Zhang, W.A. Gunderson, W.A. Cramer, M.P. Hendrich, Heme-heme interactions in the cytochrome b<sub>6</sub>f complex: EPR spectroscopy and correlation with structure, *J. Am. Chem. Soc.* 128 (2006) 14246–14247.
- [8] (a) A.I. Twigg, D. Baniulis, W.A. Cramer, M.P. Hendrich, EPR detection of an O(2) surrogate bound to heme c(n) of the cytochrome b<sub>6</sub>f complex, *J. Am. Chem. Soc.* 131 (2009) 12536–12537; (b) F. Baymann, F. Giusti, D. Picot, W. Nitschke, The ci/bH moiety in the b<sub>6</sub>f complex studied by EPR: a pair of strongly interacting hemes, *Proc. Natl. Acad. Sci. U. S. A.* 104 (2007) 519–524.
- [9] J. Alric, Y. Pierre, D. Picot, J. Lavergne, F. Rappaport, Spectral and redox characterization of the heme ci of the cytochrome b<sub>6</sub>f complex, *Proc. Natl. Acad. Sci. U. S. A.* 102 (2005) 15860–15865.
- [10] W.A. Cramer, H. Zhang, Consequences of the structure of the cytochrome b<sub>6</sub>f complex for its charge transfer pathways, *Biochim. Biophys. Acta* 1757 (2006) 339–345.
- [11] W.A. Cramer, H. Zhang, J. Yan, G. Kurisu, J.L. Smith, Transmembrane traffic in the cytochrome b<sub>6</sub>f complex, *Annu. Rev. Biochem.* 75 (2006) 769–790.
- [12] S.S. Hasan, E. Yamashita, C.M. Ryan, J.P. Whitelegge, W.A. Cramer, Conservation of lipid functions in cytochrome bc complexes, *J. Mol. Biol.* 414 (2011) 145–162.
- [13] E. Yamashita, H. Zhang, W.A. Cramer, Structure of the cytochrome b<sub>6</sub>f complex: quinone analogue inhibitors as ligands of heme c<sub>n</sub>, *J. Mol. Biol.* 370 (2007) 39–52.
- [14] G. Sainz, C.J. Carrell, M.V. Ponomarev, G.M. Soriano, W.A. Cramer, J.L. Smith, Interruption of the internal water chain of cytochrome f impairs photosynthetic function, *Biochemistry* 39 (2000) 9164–9173.
- [15] Y.I. Chi, L.S. Huang, Z.L. Zhang, J.G. Fernandez-Velasco, E.A. Berry, X-ray structure of a truncated form of cytochrome f from *Chlamydomonas reinhardtii*, *Biochemistry* 39 (2000) 7689–7701.
- [16] C.J. Carrell, B.G. Schlarb, D.S. Bendall, C.J. Howe, W.A. Cramer, J.L. Smith, Structure of the soluble domain of cytochrome f from the cyanobacterium *Phormidium laminosum*, *Biochemistry* 38 (1999) 9590–9599.
- [17] M. Ubbink, M. Ejdeback, B.G. Karlsson, D.S. Bendall, The structure of the complex of plastocyanin and cytochrome f, determined by paramagnetic NMR and restrained rigid-body molecular dynamics, *Structure* 6 (1998) 323–335.
- [18] S.E. Martinez, D. Huang, A. Szczepaniak, W.A. Cramer, J.L. Smith, Crystal structure of chloroplast cytochrome f reveals a novel cytochrome fold and unexpected heme ligation, *Structure* 2 (1994) 95–105.
- [19] S.E. Martinez, D. Huang, M. Ponomarev, W.A. Cramer, J.L. Smith, The heme redox center of chloroplast cytochrome f is linked to a buried five-water chain, *Protein Sci.* 5 (1996) 1081–1092.

- [20] S. Veit, K. Takeda, Y. Tsunoyama, D. Rexroth, M. Rogner, K. Miki, Structure of a thermophilic cyanobacterial b6f-type Rieske protein, *Acta Crystallogr. D* 68 (2012) 1400–1408.
- [21] C.J. Carrell, H. Zhang, W.A. Cramer, J.L. Smith, Biological identity and diversity in photosynthesis and respiration: structure of the lumen-side domain of the chloroplast Rieske protein, *Structure* 5 (1997) 1613–1625.
- [22] W.A. Cramer, S.E. Martinez, D. Huang, G.S. Tae, R.M. Everly, J.B. Heymann, R.H. Cheng, T.S. Baker, J.L. Smith, Structural aspects of the cytochrome b6f complex; structure of the lumen-side domain of cytochrome f, *J. Bioenerg. Biomembr.* 26 (1994) 31–47.
- [23] M. Schutz, M. Brugna, E. Lebrun, F. Baymann, R. Huber, K.O. Stetter, G. Hauska, R. Toci, D. Lemesle-Meunier, P. Tron, C. Schmidt, W. Nitschke, Early evolution of cytochrome bc complexes, *J. Mol. Biol.* 300 (2000) 663–675.
- [24] J. Yan, W.A. Cramer, Functional insensitivity of the cytochrome b6f complex to structure changes in the hinge region of the Rieske iron–sulfur protein, *J. Biol. Chem.* 278 (2003) 20925–20933.
- [25] S.S. Hasan, W.A. Cramer, On rate limitations of electron transfer in the photosynthetic cytochrome b(6)f complex, *Phys. Chem. Chem. Phys.* 14 (2012) 13853–13860.
- [26] E. Darrouzet, J.W. Cooley, F. Daldal, The cytochrome bc(1) complex and its homologue the b(6)f complex: similarities and differences, *Photosynth. Res.* 79 (2004) 25–44.
- [27] E.A. Berry, M. Guergova-Kuras, L.S. Huang, A.R. Crofts, Structure and function of cytochrome bc complexes, *Annu. Rev. Biochem.* 69 (2000) 1005–1075.
- [28] J.L. Cape, M.K. Bowman, D.M. Kramer, Understanding the cytochrome bc complexes by what they don't do. The Q-cycle at 30, *Trends Plant Sci.* 11 (2006) 46–55.
- [29] P. Mitchell, Chemiosmotic coupling in oxidative and photosynthetic phosphorylation, *Biol. Rev. Camb. Philos. Soc.* 41 (1966) 445–502.
- [30] P. Mitchell, Protonmotive redox mechanism of the cytochrome b-c1 complex in the respiratory chain: protonmotive ubiquinone cycle, *FEBS Lett.* 56 (1975) 1–6.
- [31] R. Malkin, Cytochrome-Bc(1) and cytochrome-B(6)f complexes of photosynthetic membranes, *Photosynth. Res.* 33 (1992) 121–136.
- [32] E.C. Hurt, N. Gabellini, Y. Shahak, W. Lockau, G. Hauska, Extra proton translocation and membrane-potential generation universal properties of cytochrome Bc1/B6f complexes reconstituted into liposomes, *Arch. Biochem. Biophys.* 225 (1983) 879–885.
- [33] H. Zhang, J.P. Whitelegge, W.A. Cramer, Ferredoxin:NADP+ oxidoreductase is a subunit of the chloroplast cytochrome b6f complex, *J. Biol. Chem.* 276 (2001) 38159–38165.
- [34] A.R. Crofts, M. Guergova-Kuras, R. Kuras, N. Ugulava, J. Li, S. Hong, Proton-coupled electron transfer at the Q(o) site: what type of mechanism can account for the high activation barrier? *Biochim. Biophys. Acta* 1459 (2000) 456–466.
- [35] A.R. Crofts, Z.G. Wang, How rapid are the internal reactions of the ubiquinol-cytochrome-C2 oxidoreductase, *Photosynth. Res.* 22 (1989) 69–87.
- [36] C. Lange, J.H. Nett, B.L. Trumpower, C. Hunte, Specific roles of protein–phospholipid interactions in the yeast cytochrome bc1 complex structure, *EMBO J.* 20 (2001) 6591–6600.
- [37] D. Xia, K.P. Deng, H. Kim, A. Kachurin, C.A. Yu, L. Yu, J. Deisenhofer, Crystallographic analysis of core proteins of cytochrome b/c1 complex — implication to the structure and function of mitochondrial processing peptidase, *Biophys. J.* 72 (1997), (Th363–Th363).
- [38] X. Gao, X. Wen, L. Esser, B. Quinn, L. Yu, C.A. Yu, D. Xia, Structural basis for the quinone reduction in the bc1 complex: a comparative analysis of crystal structures of mitochondrial cytochrome bc1 with bound substrate and inhibitors at the Qi site, *Biochemistry* 42 (2003) 9067–9080.
- [39] W.A. Cramer, S.S. Hasan, E. Yamashita, The Q cycle of cytochrome bc complexes: a structure perspective, *Biochim. Biophys. Acta* 1807 (2011) 788–802.
- [40] A.M. Seddon, P. Curnow, P.J. Booth, Membrane proteins, lipids and detergents: not just a soap opera, *Biochim. Biophys. Acta* 1666 (2004) 105–117.
- [41] L. Adamian, H. Naveed, J. Liang, Lipid-binding surfaces of membrane proteins: evidence from evolutionary and structural analysis, *Biochim. Biophys. Acta* 1808 (2011) 1092–1102.
- [42] J. Liang, H. Naveed, D. Jimenez-Morales, L. Adamian, M. Lin, Computational studies of membrane proteins: models and predictions for biological understanding, *Biochim. Biophys. Acta* 1818 (2012) 927–941.
- [43] J.M. Vergis, M.D. Purdy, M.C. Wiener, A high-throughput differential filtration assay to screen and select detergents for membrane proteins, *Anal. Biochem.* 407 (2010) 1–11.
- [44] S. Nussberger, K. Dorr, D.N. Wang, W. Kuhlbrandt, Lipid–protein interactions in crystals of plant light-harvesting complex, *J. Mol. Biol.* 234 (1993) 347–356.
- [45] J.P. Cartailier, H. Luecke, X-ray crystallographic analysis of lipid–protein interactions in the bacteriorhodopsin purple membrane, *Annu. Rev. Biophys. Biomol. Struct.* 32 (2003) 285–310.
- [46] P.V. Escriba, P.B. Wedegaertner, F.M. Goni, O. Vogler, Lipid–protein interactions in GPCR-associated signaling, *Biochim. Biophys. Acta Biomembr.* 1768 (2007) 836–852.
- [47] R.K. Hite, Z.L. Li, T. Walz, Principles of membrane protein interactions with annular lipids deduced from aquaporin-0 2D crystals, *EMBO J.* 29 (2010) 1652–1658.
- [48] L. Qin, C. Hiser, A. Mulichak, R.M. Garavito, S. Ferguson-Miller, Identification of conserved lipid/detergent-binding sites in a high-resolution structure of the membrane protein cytochrome c oxidase, *Proc. Natl. Acad. Sci. U. S. A.* 103 (2006) 16117–16122.
- [49] L. Qin, M.A. Sharpe, R.M. Garavito, S. Ferguson-Miller, Conserved lipid-binding sites in membrane proteins: a focus on cytochrome c oxidase, *Curr. Opin. Struct. Biol.* 17 (2007) 444–450.
- [50] H. Zhang, G. Kurisu, J.L. Smith, W.A. Cramer, A defined protein–detergent–lipid complex for crystallization of integral membrane proteins: the cytochrome b6f complex of oxygenic photosynthesis, *Proc. Natl. Acad. Sci. U. S. A.* 100 (2003) 5160–5163.
- [51] D. Baniulis, E. Yamashita, H. Zhang, S.S. Hasan, W.A. Cramer, Structure–function of the cytochrome b6f complex, *Photochem. Photobiol.* 84 (2008) 1349–1358.
- [52] H. Zhang, W.A. Cramer, Problems in obtaining diffraction-quality crystals of hetero-oligomeric integral membrane proteins, *J. Struct. Funct. Genomics* 6 (2005) 219–223.
- [53] H. Zhang, W.A. Cramer, Purification and crystallization of the cytochrome b6f complex in oxygenic photosynthesis, *Methods Mol. Biol.* 274 (2004) 67–78.
- [54] D. Baniulis, H. Zhang, T. Zakharova, S.S. Hasan, W.A. Cramer, Purification and crystallization of the cyanobacterial cytochrome b6f complex, *Methods Mol. Biol.* 684 (2011) 65–77.
- [55] C. Breyton, C. Tribet, J. Olive, J.P. Dubacq, J.L. Popot, Dimer to monomer conversion of the cytochrome b(6)f complex — causes and consequences, *J. Biol. Chem.* 272 (1997) 21892–21900.
- [56] Y. Pierre, C. Breyton, D. Kramer, J.L. Popot, Purification and characterization of the cytochrome B(6)f complex from *Chlamydomonas reinhardtii*, *J. Biol. Chem.* 270 (1995) 29342–29349.
- [57] S.S. Hasan, W.A. Cramer, Lipid functions in cytochrome bc complexes: an odd evolutionary transition in a membrane protein structure, *Philos. Trans. R. Soc. Lond. B Biol. Sci.* 367 (2012) 3406–3411.
- [58] (a) F. Zito, G. Finazzi, R. Delosme, W. Nitschke, D. Picot, F.A. Wollman, The Qo site of cytochrome b6f complexes controls the activation of the LHCl1 kinase, *EMBO J.* 18 (1999) 2961–2969;
- (b) B. Schoepp-Cothenet, R. van Lis, A. Atteia, F. Baymann, L. Capowicz, A.L. Ducluzeau, S. Duval, F. ten Brink, M.J. Russell, W. Nitschke, On the universal core of bioenergetics, *Biochim. Biophys. Acta* 1827 (2013) 79–93.
- [59] T. Kallas, R. Malkin, Isolation and characterization of genes for cytochrome b6/f complex, *Methods Enzymol.* 167 (1988) 779–794.
- [60] T. Kallas, S. Spiller, R. Malkin, Characterization of two operons encoding the cytochrome b6-f complex of the cyanobacterium *Nostoc* PCC 7906. Highly conserved sequences but different gene organization than in chloroplasts, *J. Biol. Chem.* 263 (1988) 14334–14342.
- [61] W. Majeran, F.A. Wollman, O. Vallon, Evidence for a role of ClpP in the degradation of the chloroplast cytochrome b(6)f complex, *Plant Cell* 12 (2000) 137–150.
- [62] Y. Choquet, D.B. Stern, K. Wostrikoff, R. Kuras, J. Girard-Bascou, F.A. Wollman, Translation of cytochrome f is autoregulated through the 5' untranslated region of petA mRNA in *Chlamydomonas* chloroplasts, *Proc. Natl. Acad. Sci. U. S. A.* 95 (1998) 4380–4385.
- [63] R. Kuras, S. Buschlen, F.A. Wollman, Maturation of pre-apocytochrome-F in-vivo — a site-directed mutagenesis study in *Chlamydomonas reinhardtii*, *J. Biol. Chem.* 270 (1995) 27797–27803.
- [64] R. Kuras, C. de Vitry, Y. Choquet, J. Girard-Bascou, D. Culler, S. Buschlen, S. Merchant, F.A. Wollman, Molecular genetic identification of a pathway for heme binding to cytochrome b(6), *J. Biol. Chem.* 272 (1997) 32427–32435.
- [65] R. Kuras, F.A. Wollman, The assembly of cytochrome B(6)/F complexes — an approach using genetic-transformation of the green-alga *Chlamydomonas reinhardtii*, *EMBO J.* 13 (1994) 1019–1027.
- [66] C. Lemaire, J. Girard-Bascou, F.A. Wollman, P. Bennoun, Studies on the cytochrome B6/F complex. 1. Characterization of the complex subunits in *Chlamydomonas reinhardtii*, *Biochim. Biophys. Acta* 851 (1986) 229–238.
- [67] R. Kuras, F.A. Wollman, P. Joliet, Conversion of cytochrome-F to a soluble form in-vivo in *Chlamydomonas reinhardtii*, *Biochemistry* 34 (1995) 7468–7475.
- [68] F.A. Wollman, R. Kuras, Y. Choquet, Epistatic effects in thylakoid protein synthesis: the example of cytochrome f, photosynthesis: from light to biosphere, *III* (1995) 737–742.
- [69] F. Zito, R. Kuras, Y. Choquet, H. Kossel, F.A. Wollman, Mutations of cytochrome b(6) in *Chlamydomonas reinhardtii* disclose the functional significance for a proline to leucine conversion by petB editing in maize and tobacco, *Plant Mol. Biol.* 33 (1997) 79–86.
- [70] M. el-Demerdash, J. Salnikow, J. Vater, Evidence for a cytochrome f-Rieske protein subcomplex in the cytochrome b6f system from spinach chloroplasts, *Arch. Biochem. Biophys.* 260 (1988) 408–415.
- [71] S. Schwenkert, J. Legen, T. Takami, T. Shikanai, R.G. Herrmann, J. Meurer, Role of the low-molecular-weight subunits PetL, PetG, and PetN in assembly, stability, and dimerization of the cytochrome b6f complex in tobacco, *Plant Physiol.* 144 (2007) 1924–1935.
- [72] W.A. Cramer, J. Yan, H. Zhang, G. Kurisu, J.L. Smith, Structure of the cytochrome b6f complex: new prosthetic groups, Q-space, and the 'hors d'oeuvres hypothesis' for assembly of the complex, *Photosynth. Res.* 85 (2005) 133–143.
- [73] L.I. Krishtalik, W.A. Cramer, On the physical basis for the cis-positive rule describing protein orientation in biological-membranes, *FEBS Lett.* 369 (1995) 140–143.
- [74] D. Schneider, S. Berry, P. Rich, A. Seidler, M. Rogner, A regulatory role of the PetM subunit in a cyanobacterial cytochrome b6f complex, *J. Biol. Chem.* 276 (2001) 16780–16785.
- [75] D. Schneider, T. Volkmer, M. Rogner, PetG and PetN, but not PetL, are essential subunits of the cytochrome b6f complex from *Synechocystis* PCC 6803, *Res. Microbiol.* 158 (2007) 45–50.
- [76] F. Zito, G. Finazzi, P. Joliet, F.A. Wollman, Glu78, from the conserved PEWY sequence of subunit IV, has a key function in cytochrome b6f turnover, *Biochemistry* 37 (1998) 10395–10403.
- [77] S. Izrailov, A.R. Crofts, E.A. Berry, K. Schulten, Steered molecular dynamics simulation of the Rieske subunit motion in the cytochrome bc(1) complex, *Biophys. J.* 77 (1999) 1753–1768.
- [78] D. Victoria, R. Burton, A.R. Crofts, Role of the -PEWY-glutamate in catalysis at the Q(o)-site of the Cyt bc(1) complex, *Biochim. Biophys. Acta* 1827 (3) (March 2013) 365–386.
- [79] S.R. Solmaz, C. Hunte, Structure of complex III with bound cytochrome c in reduced state and definition of a minimal core interface for electron transfer, *J. Biol. Chem.* 283 (2008) 17542–17549.

- [80] J.D. Rochaix, Regulation of photosynthetic electron transport, *Biochim. Biophys. Acta* 1807 (2011) 375–383.
- [81] S. Lemeille, A. Willig, N. Depege-Fargeix, C. Delessert, R. Bassi, J.D. Rochaix, Analysis of the chloroplast protein kinase Stt7 during state transitions, *PLoS Biol.* 7 (2009) 664–675.
- [82] N. Depege, S. Bellaïf, J.D. Rochaix, Role of chloroplast protein kinase Stt7 in LHClI phosphorylation and state transition in *Chlamydomonas*, *Science* 299 (2003) 1572–1575.
- [83] (a) W.A. Cramer, S. Savikhin, J.S. Yan, E. Yamashita, The enigmatic chlorophyll a molecule in the cytochrome b(6)f complex, chloroplast: basics and applications, 31 (2010) 89–93;
- (b) F. Zito, J. Vinh, J.L. Popot, G. Finazzi, Chimeric fusions of subunit IV and PetL in the b6f complex of *Chlamydomonas reinhardtii*: structural implications and consequences on state transitions, *J. Biol. Chem.* 277 (14) (Apr 5 2002) 12446–12455, (Electronic publication ahead of print 2002 Jan 16).
- [84] D.L. Dexter, A theory of sensitized luminescence in solids, *J. Chem. Phys.* 21 (1953) 836–850.
- [85] N. Dashdorj, H. Zhang, H. Kim, J. Yan, W.A. Cramer, S. Savikhin, The single chlorophyll a molecule in the cytochrome b6f complex: unusual optical properties protect the complex against singlet oxygen, *Biophys. J.* 88 (2005) 4178–4187.
- [86] J. Yan, N. Dashdorj, D. Baniulis, E. Yamashita, S. Savikhin, W.A. Cramer, On the structural role of the aromatic residue environment of the chlorophyll a in the cytochrome b6f complex, *Biochemistry* 47 (2008) 3654–3661.
- [87] M. Iwai, K. Takizawa, R. Tokutsu, A. Okamuro, Y. Takahashi, J. Minagawa, Isolation of the elusive supercomplex that drives cyclic electron flow in photosynthesis, *Nature* 464 (2010) 1210–1213.
- [88] P. Jordan, P. Fromme, H.T. Witt, O. Klukas, W. Saenger, N. Krauss, Three-dimensional structure of cyanobacterial photosystem I at 2.5 angstrom resolution, *Nature* 411 (2001) 909–917.
- [89] Y. Umena, K. Kawakami, J.R. Shen, N. Kamiya, Crystal structure of oxygen-evolving photosystem II at a resolution of 1.9 Å, *Nature* 473 (2011) 55–60.
- [90] A. Guskov, J. Kern, A. Gabdulkhakov, M. Broser, A. Zouni, W. Saenger, Cyanobacterial photosystem II at 2.9-angstrom resolution and the role of quinones, lipids, channels and chloride, *Nat. Struct. Mol. Biol.* 16 (2009) 334–342.
- [91] J. Standfuss, A.C. Terwisscha van Scheltinga, M. Lamborghini, W. Kuhlbrandt, Mechanisms of photoprotection and nonphotochemical quenching in pea light-harvesting complex at 2.5 Å resolution, *EMBO J.* 24 (2005) 919–928.
- [92] G. von Jagow, T.A. Link, Use of specific inhibitors on the mitochondrial bc1 complex, *Methods Enzymol.* 126 (1986) 253–271.
- [93] A.R. Crofts, M. Guergova-Kuras, L. Huang, R. Kuras, Z. Zhang, E.A. Berry, Mechanism of ubiquinol oxidation by the bc(1) complex: role of the iron sulfur protein and its mobility, *Biochemistry* 38 (1999) 15791–15806.
- [94] A.R. Crofts, B. Barquera, R.B. Gennis, R. Kuras, M. Guergova-Kuras, E.A. Berry, Mechanism of ubiquinol oxidation by the bc(1) complex: different domains of the quinol binding pocket and their role in the mechanism and binding of inhibitors, *Biochemistry* 38 (1999) 15807–15826.
- [95] X. Gao, X. Wen, C. Yu, L. Esser, S. Tsao, B. Quinn, L. Zhang, L. Yu, D. Xia, The crystal structure of mitochondrial cytochrome bc1 in complex with famoxadone: the role of aromatic–aromatic interaction in inhibition, *Biochemistry* 41 (2002) 11692–11702.
- [96] G.J. Kleywegt, M.R. Harris, J.Y. Zou, T.C. Taylor, A. Wahlby, T.A. Jones, The Uppsala Electron-Density Server, *Acta Crystallogr. D Biol. Crystallogr.* 60 (2004) 2240–2249.